

# Identify As A Human Does: A Pathfinder of Next-Generation Anti-Cheat Framework for First-Person Shooter Games

Jiayi Zhang<sup>✉</sup>, Chenxin Sun<sup>✉</sup>, Yue Gu<sup>✉</sup>, Qingyu Zhang<sup>✉</sup>, Jiayi Lin<sup>✉</sup>,  
Xiaojiang Du<sup>✉</sup>, *Fellow, IEEE*, and Chenxiong Qian<sup>✉</sup>, *Member, IEEE*

**Abstract**—The gaming industry has experienced substantial growth, but cheating in online games poses a significant threat to the integrity of the gaming experience. Cheating, particularly in first-person shooter (FPS) games, can lead to substantial losses for the game industry. Existing anti-cheat solutions have limitations, such as client-side hardware constraints, security risks, server-side unreliable methods, and both-sides suffer from a lack of comprehensive real-world datasets. To address these limitations, the paper proposes HAWK, a server-side FPS anti-cheat framework for the popular game CS:GO. HAWK utilizes machine learning techniques to mimic human experts' identification process, leverages novel multi-view features, and is equipped with a well-defined workflow. HAWK is evaluated with the first large and real-world datasets containing multiple cheat types and cheating sophistication, and it exhibits promising efficiency and acceptable overheads, shorter ban times, higher recall and similar false positive rate compared to the in-use anti-cheat, and the ability to capture cheaters who evaded official inspections.

**Index Terms**—Game security, anti-cheat, intrusion detection, machine learning.

## I. INTRODUCTION

THE gaming industry has experienced substantial growth recently, with the global games market generating \$187.7 billion in 2024 and projected to generate \$213.3 billion by 2027 [1]. However, cheating in online games poses a significant threat to the integrity of gaming experiences and disrupts gameplay balance. In 2023 alone, cheating led to an estimated \$29 billion losses, with 78% of players discouraged from playing due to cheating [2]. In particular, first-person shooter (FPS) games, which account for 20.9% of total game sales [3], are particularly targeted by cheat developers because their stringent latency requirements make key computations on the client side, creating fertile ground for cheats to exploit.

Jiayi Zhang, Chenxin Sun, Yue Gu, Qingyu Zhang, Jiayi Lin, and Chenxiong Qian are with the School of Computing and Data Science, The University of Hong Kong, Hong Kong 999077, China (e-mail: cqian@cs.hku.hk). Jiayi Zhang and Chenxin Sun contributed equally to this research.

Xiaojiang Du is with the Department of Electrical and Computer Engineering, Stevens Institute of Technology, NJ 07030, USA.

Received 6 March 2025; revised 24 August 2025; accepted 10 November 2025. Date of publication <TBD HERE>; date of current version <TBD HERE>. This work is partially supported by the NSFC for Young Scientists of China (No.62202400) and the RGC for Early Career Scheme (No.27210024). The associate editor coordinating the review of this article and approving it for publication was Prof. Abderrahim Benslimane. (*Corresponding author: Chenxiong Qian.*)

This paper has supplementary downloadable material available at <http://ieeexplore.ieee.org>., provided by the authors. The material includes detailed feature designs, experimental settings, additional evaluation details. Contact [brucejiayi@connect.hku.hk](mailto:brucejiayi@connect.hku.hk) for further questions about this work.

Digital Object Identifier 10.1109/TIFS.<TBD HERE>

The most prevalent forms of cheating involve the use of *aimbots* to aid aiming and *wallhacks* to reveal opponents' positions, thus compromising game integrity [4], [5], [6].

Realizing the critical importance of game security [7], both academia and industry have proposed many anti-cheats solutions, applied either on the client side [6], [8], [9] or server side [10], [11], [12], [13]. However, current solutions have the following limitations.

Client-side solutions face hardware constraints, security and privacy concerns, or unacceptable system overheads. Two state-of-the-art systems [6], [9] require a specific Trusted Execution Environment (TEE), Intel SGX. This dependence on particular hardware, which was deprecated in 2021 [14], [15], limits the compatibility and practicality for industrial use. Some industrial solutions [16], [17], [18] involve scanning hard drives and gaining root privileges, posing risks of unauthorized access and personal data leakage [19], [20], [21]. Vulnerabilities, e.g., RCE exploits [22] and CVEs [23], [24], [25], [26], demonstrate the potential for system instability and privacy breaches. And most client-side works rely on concurrent surveillance [9], [8] leading to increased client-side overheads, or frequent patching to counter varying cheat signatures [16], [17], [18], [6], which requires extra engineering efforts and is considered to be less effective [13] since it only identifies known and deprecated cheats. Importantly, client-side data and decision results are unreliable and easily tampered with [27], [28], [29], [13]. Thus, the industry has shifted towards server-side anti-cheat solutions [27], [28].

However, existing server-side solutions use basic features and have low recall and accuracy. For instance, previous works [10], [11], [13], [30], [31] use naive features like winning rates, playtime, or count shots on an invisible bait which are insufficient or inapplicable for detecting today's complex cheats or specific cheat types. These works leverage thresholds to classify, which is not robust enough for practical use, especially in noise-rich, real-world datasets. Additionally, some commercial anti-cheats integrate such server-side approaches [16]. Yet, they show low recall and accuracy, with extended ban cycles and increasing community grievances [32], [33]. Incidents like the 2024 APEX Legends Tournament hack [34] and the study [30] highlight the ineffectiveness of existing commercial anti-cheats, e.g., EAC [16] and VAC [18].

More broadly, prior research on anti-cheat techniques suffers from the lack of comprehensive real-world datasets, with most studies relying on limited or synthetic data [6], [9], [10], [11], [12], [13], which are hard to capture diverse cheating scenarios and varying levels of sophistication (explained in **Section II-B**). This could result in performance degradation or

TABLE I: Detection works comparison. ‘Availability’: public availability of technical details (T), source code (C), and datasets (D), **red** and **green** indicate unavailable and available. ‘Dynamic Tuning’: ability to adjust different anti-cheat demands (e.g., prioritize different metrics, introduced in Section V-D) without retraining the entire system. ‘Data Extraction-Game Coupling Degree’: difficulty of acquiring the game’s raw data, ‘high coupling’ indicates the process is highly coupled with the game logic (e.g., modify engine, hooking process), making it challenging to generalize or reuse across different game versions.

Side	Method	Work(s)	Availability	Detection Feature Comprehensiveness	Data Extraction-Game Coupling Degree	Real-world Functionality				
						Dataset	Deployment Constraint	Robustness	Dynamic Tuning	Performance
Client	ML-based	[6]	T, C, D	Single aspect & data type	High Coupling	SSL <sup>1</sup>	TEE (Intel SGX)	Unknown	✗	Unknown <sup>2</sup>
	Commercial signature-based	[16], [17], [18], [35], [36]	T, C, D	Unknown	High Coupling	Real-world	OS and kernel drivers	Unknown	Unknown	Low recall, acceptable FPR
Server	Statistical/Threshold-based	[10], [11], [13], [30], [31]	T, C, D	Single aspect & data type	High Coupling	SSL	Concurrent overheads	Unknown	✗	Unknown
	ML-based	[12]	T, C, D	Single aspect & data type	High Coupling	SSL	Concurrent overheads	Unknown	✗	Unknown
	HAWK		T, C, D	Multiple aspects & data types	Low Coupling	Real-world	None	CE <sup>3</sup> N <sup>4</sup>	✓	High recall, similar FPR

<sup>1</sup>SSL: Simulated, small-scale, low complexity; <sup>2</sup>Unknown: Never been tested or disclosed; <sup>3</sup>CE: Robust to cheat evolution (an adversarial attack in Section VI-G); <sup>4</sup>N: Robust to noise.

even failure in complex real-world scenarios.

To address the aforementioned limitations, we propose HAWK, a server-side approach designed to analyze data transmitted to the server, thereby avoiding the inherent limitations of client-side solutions. HAWK introduces a comprehensive set of multi-view features and a robust framework to meticulously monitor players’ points of view, statistics, and behavioral consistencies. This approach includes a corresponding workflow that aims to shorten the ban cycle and considers the occurrence of false positives. HAWK achieves high detection recall and acceptable accuracy in large real-world data sets with varying levels of sophistication of cheating. Table I listed the comparison between HAWK and other detection methods.

The key innovation of HAWK lies in its ability to mimic how human experts identify cheaters by focusing on three dimensions: analyzing the player’s point of view, statistically evaluating the player’s performance, and assessing the player’s gaming sense and performance consistency. Building on these dimensions, we design structured and temporal features that precisely describe player behaviors. These features are selected from hundreds of candidates to ensure that they effectively represent diverse behavioral patterns. HAWK replicates the human identification process by leveraging machine learning techniques, including Long Short-Term Memory (LSTM) with attention mechanisms, ensemble learning, and deep neural networks, each tailored to specific aspects of the analysis. HAWK addresses the challenges of integrating heterogeneous data structures and dynamically adjusting anti-cheating priorities by developing a dedicated integration subsystem, MVIN.

We evaluate HAWK on a mainstream FPS game, CS:GO. To the best of our knowledge, this paper is the first server-side work using a substantial volume of real-world datasets with different cheat types and levels of sophistication, making HAWK and the datasets more convincing for industrial use. Specifically, our dataset includes 2,979 *aimbots* and 2,971 *wallhacks*, totaling 56,041 players. The scale of the dataset has increased by two orders of magnitude compared to the state-of-the-art work [6]. HAWK achieves at most 84% recall and 80% accuracy in detecting *aimbots* and *wallhacks*. HAWK outperforms baselines in the separate comparisons across different subsystems, given HAWK’s diverse input data structures. It successfully identifies cheaters who had evaded previous detections and those who were never caught by official sys-

tems. We created a demo website<sup>1</sup> to showcase some escapees’ illegal actions. HAWK validates its robustness against cheat evolution (introduced in Section VI-G) in real-world scenarios and showcases acceptable overheads. We particularly discuss HAWK’s generalizability in Section VII. The contributions of our work are summarized below.

- Innovative anti-cheat observations and feature designs.
- Novel framework HAWK and a supporting workflow.
- Real-world *data* evaluations with strong performance.
- Open-source HAWK and dataset<sup>2</sup> for future research.

## II. BACKGROUND

The section introduces anti-cheat, cheating techniques, the current state of cheating, and the replay design in FPS games.

### A. Server-Side and Client-Side Anti-Cheat

Client-side anti-cheats focus on data, process, and hardware protection [9], [8], or detection by examining the existing cheats’ signatures [16], [17] or classifying through aiming behavior [6]. Yet, attackers can bypass it with higher privileges, by sniffing the detection report through side-channel attack [37] and altering them in the transport layer, or by changing the program’s signature [38]. Server-side anti-cheats [10], [11], [12], [39], [13], [31] emphasize data analysis and anomaly detection. Although the data might be altered on the client, they must secure victory by outperforming other players. Thus, detecting cheats on the server is easier because it records all clients’ final-state actions influencing the gameplay. But the prior works have the limitations mentioned in Section I.

### B. Cheating in FPS Games

Wallhack and aimbot are the two most prevalent types of cheats in FPS games [40]. Both types of cheats are mainly done by accessing the client’s memory data or image information. **Wallhack** enables players to visually penetrate obstructions like walls, which allows players to spot opponents across the map and effortlessly track their movements, providing a significant tactical advantage. **Aimbot** assists a player’s aims and shots so that the cheaters gain transcendent

<sup>1</sup>Demo website: <https://hawk-anticheat.github.io/>.

<sup>2</sup>Public repository and dataset: [10.6084/m9.figshare.25940818](https://doi.org/10.6084/m9.figshare.25940818). Ethics considerations are shown in Supplemental Material A.

precision and reaction speed. *Aimbot*'s functionality can be customized according to player preference, allowing one to obtain different aiming performance, ranging from brutal-force aims to smooth aims like human [6]. *Aimbot* can be subdivided into *pure aimbot* (the primitive *aimbot*), *triggerbot* (auto-shoot only when the cross-hair is on the opponent), *micro-settings* (counteract recoil with Hotkeys), and *computer-vision-based aimbot* (aim with object detection models). In our paper, *aimbot* refers to all aforementioned subcategories. Cheating provides different levels of sophistication [21]. The cheater might cheat cautiously, pretending to be a normal player, switching the cheat on and off, or cheating unabashedly with different configurations, various brands of cheating software, and categories. However, cheaters' behaviors will always differ from the normal players [6]. Thus, cheaters must outperform the average to gain unfair advantages. This is bound to create anomalies at the data level and therefore should be identifiable by models. Our evaluations in Section VI include different levels of cheating sophistication.

### C. Replay System and Replay File

**Replay system** is a dynamic toolset for player interaction with recorded content post-game and has been extensively adopted in notable FPS games. Unlike video recordings, this system enables users to explore various perspectives, adjust camera angles, and control playback speed for analysis by reconstructing the match with the *replay file*. **Replay file** refers to a comprehensive record of a match, encapsulated in a unique data format that can be interpreted by the *replay system*. **Demo** denotes the *replay file* in CS:GO. HAWK innovatively utilizes *demo* to extract data and avoid concurrent overheads on the server. We believe the *replay file* can be used as a novel data source for FPS server-side anti-cheat.

## III. OVERVIEW

This section provides the key observations on the human experts' identification process and the workflow of HAWK.

### A. Fact Observations

Although the anti-cheat tasks are still challenging for automation systems in FPS games, the illegal activities are identifiable for seasoned human players [41]. Therefore, by harnessing such inspiration, we discovered three observations that human experts always focus on to identify cheaters.

**Observation 1 (OBS.1).** Review a player's point-of-view (POV).

Akin to watching a player's game replay unfold over time, this review process involves analyzing various in-game behaviors, such as aim and shot, positioning and movement, and the in-game economy management and props utilization. These behaviors can provide temporal insights into the legitimacy of a player's gameplay.

**Observation 2 (OBS.2).** Conduct an in-depth analysis of a player's statistical data.

Cheaters often exhibit statistical anomalies that set them apart from normal players. These anomalies include abnormally high accuracy and eliminations, a low death rate, and a high number of kills made through obstacles, etc. These statistical deviations serve as strong indicators of cheating.

**Observation 3 (OBS.3).** Examine the consistency between a player's game sense and combat performance.

A player requires substantial game experience to have better performances, which results in a positive correlation between a player's game sense and their performance. Thus, the inconsistency between the two aforementioned factors indicates potential cheating. For instance, if a player moves like a rookie but shoots and aims incredibly accurately, it is suspicious.

### B. Workflow

Figure 1 illustrates HAWK's interlinked workflow, which enhances the system's robustness and provides a dynamic solution to multi-type cheat detection (discussed in Section VI-G).

- ① **Preprocessing.** The multi-view features are extracted from the parsed *demo* and then annotated for training. We discuss the feature constructions in Section IV.
- ② **HAWK deployment.** HAWK utilizes the extracted features as inputs for its subsystems REVPOV (Section V-A), REVSTATS (Section V-B), and EXSPC (Section V-C) to mimic human identification process, respectively. The outputs are incorporated into MVIN subsystem (Section V-D) that presents a final cheating report. HAWK's evaluation results in Section VI are based on the results after this step.
- ③ **Game Master (GM) team verification.** Given the potential personal assets tied to a player's account, a ban should not be issued solely based on an algorithmic verdict. It is imperative to provide substantial evidence before initiating such an action. Hence, the final verdict requires GMs' verification to avoid false bans. This step is to display the entire process from data collection to the ban.
- ④ **Archiving and data updates.** Upon the affirmation of cheating, the relevant *demos* are added to the banned databases and ready for retraining that may introduce novel patterns.

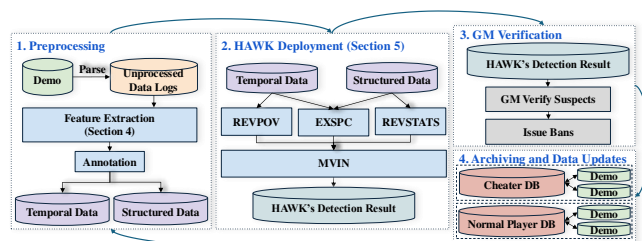


Fig. 1: Cyclical workflow of HAWK.

#### IV. HAWK'S FEATURE DESIGN

The feature design is one of our contributions. This section introduces the construction of structured features, temporal features, and the classification of sense and performance features. These features are selected among hundreds of our designed naive features and intended to be comprehensive representations of the three aspects of human identification of cheating in Section III-A to overcome the challenge of the potentially biased classifications brought by the monospecific features in the prior works mentioned in Section I.

##### A. Structured Features

Structured features are single-value data calculated with well-designed algorithms to represent integrated in-game behavioral information per match and ensure time complexity. This section describes the components of structured features and visualizes the structured feature differences between normal players and cheaters.

1) *Structured Features Construction*: The structured features for HAWK are categorized into four main categories that comprise 28 features. For the sake of brevity and coherence, only the introduction of categories is outlined below. A meticulous breakdown is shown in Supplemental Material C.

- **Aiming features** represents the efficiency and efficacy of aims. We break down the aiming process into three moments (initial spot, first-time fire, and first-time hit) and two stages (reaction and adjustment). We extract different elapsed durations and angle variations with statistical representations (e.g., average or variance) to indicate the player's different performances within a match. For example, the average of *reaction duration* reflects a player's level of reaction speed, and the variance of that denotes the distribution of the reaction duration. Typically, in terms of the reaction stage, normal players obtain a higher mean value and more diverse variance compared with cheaters.
- **Firing features** reflects shot proficiency. For example, the *hit group distribution variance* describes the dispersion of body part that suffers damage for the current player in a match. Most cheaters with *aimbot* prefer to lock on specific *hit group* (i.e., *head*) to achieve faster elimination.
- **Elimination features** emphasizes metrics related to in-game kill events. For example, the *occluder-penetration index* is a weighted index that reflects the extent of the average occluder-penetration eliminations (e.g., eliminate the opponent behind walls or smoke) conducted by the player. In terms of the cheaters exploiting *wallhacks*, this index is more significant than the normal players'.
- **Props utilization features** captures a player's adeptness at using in-game auxiliary and offensive props like flashbang, grenades, etc. For instance, the *props utilization index* denotes how frequently a player utilizes auxiliary and offensive props such as incendiaries and smoke grenades. This can help distinguish a player's familiarity with the game and their skillfulness.

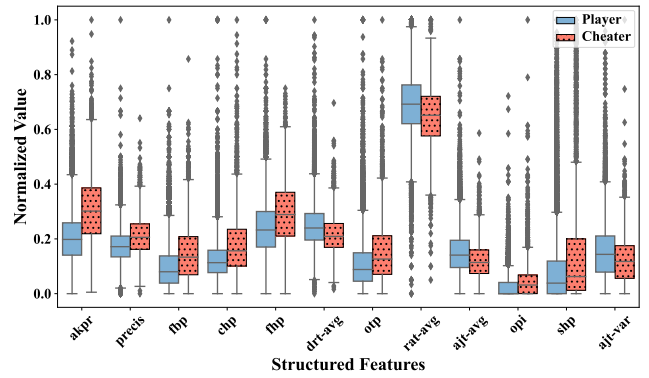


Fig. 2: Box plots of comparative visualization between honest players and cheaters on top-12 structured features under the Mann-Whitney U test with distinction descending order.

2) *Structured Data Comparative Visualization*: Figure 2 offers a box-plot on structured features to analyze between honest players and cheaters comparatively. Each feature on the x-axis (we select top-12 features for illustration purposes) is ordered based on the outcomes of the Mann-Whitney U test, with the leftmost features, such as *akpr* (introduced in Supplemental Material C), marking pronounced disparities between the two groups. This implies that features towards the left end, showcased by their lower p-values, are more distinguishable, whereas those on the right are less so. The y-axis is normalized values between 0 and 1. The box plots, distinguished by light blue for honest players and hatched red for cheaters, provide insights into the median, interquartile range, and outlier distributions. In which, diamond shapes represent outliers, emphasizing the spread and distribution of data across the features. Despite considering dimensionality reduction techniques, such as PCA (Supplemental Material Figure 4), empirical tests show an optimal performance when all 28 features were employed. Therefore, cheaters often exhibit deviations in their static data compared to normal players. Even when cheaters deliberately attempt to conceal their behavior, the subtle differences tend to accumulate over time and reveal disparities statistically.

##### B. Temporal Features

Temporal features are derived in the time domain. Each temporal data tuple is the state information (e.g., coordinates, view directions, events, etc.) associated with the present *tick*. Where *tick* denotes the smallest unit of time in the game.

1) *Temporal Features Construction*: According to different in-game behaviors, temporal features are segmented into three main categories and subdivided into seven specific types. Supplemental Material D lists elaborate descriptions.

- **Engagement features** describes in-game engagement events, which are subcategorized into five types as follows.
  - **Damage features** indicate damage-inflicting events, including the occurring *tick*, the attacker's and victim's locations, view directions, weapons, damage value, etc.

- **Auxiliary props features** related to auxiliary props-utilization events (e.g., flashbang), including the deploy *tick*, victim’s affected duration, etc.
  - **Offensive props features** related with events involving props that aid the attack (e.g., grenade, incendiary, etc.) including the deploy and destroy *ticks*, the props’ type and coordinates, etc.
  - **Elimination features** describes kill-related events, including the occurring *tick*, attacker’s weapon and location, victim’s location and view direction, etc.
  - **Weapon fire features** denotes firing-related occurrences, including the occurring *tick*, the weapon information, the shooter’s location and view direction, etc.
- **Movement features** represents in-game positioning, mobility, and boolean flags per *tick*. For instance, coordinates, view directions, velocities in three dimensions, flags that indicate if the player is ducking, blinded, reloading, etc.
  - **Economy features** reflects in-game financial aspects. For example, they include the equipment value and balance per *round* for each player.

2) *Temporal Data Comparative Visualization*: **Figure 3** comparatively analyzes the temporal features between cheaters and normal players across one *round*. Where **round** denotes the unit determining each win-loss outcome. One match has multiple rounds, and the players who win more rounds are the winners. In this example, there are four differences between cheaters and normal players. First, since the cheaters illegally acquire their opponents’ position, the timing of cheaters’ firing (pink) and engaging (red) highly overlap (a). Second, normal players stay on guard (blue) irregularly to check for potential enemy locations, whereas cheaters are often on guard just before engagement (b). Third, normal players deploy props (orange) to gain a gunfighting or positional advantage, whereas cheaters rarely do so because they already have illegal advantages (c). Fourth, cheaters are rarely vulnerable (yellow) during the fire or engagement because they know the enemy’s location and therefore can circumvent it in advance (d).

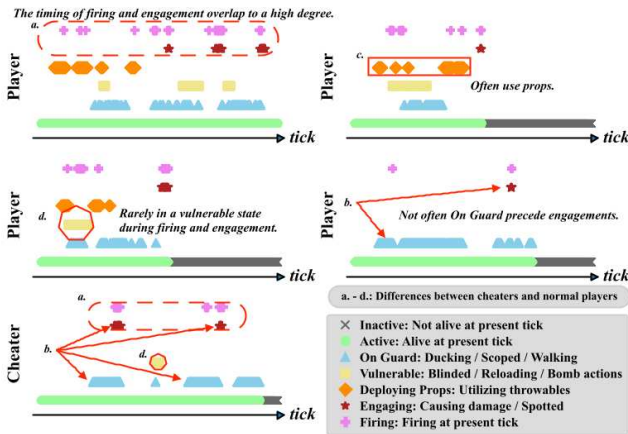


Fig. 3: Comparative behavioral visualization between honest players and cheaters with respect to time scales.

### C. Sense and Performance Features

Sense and performance features are derived from the previous subsections. Supplemental Material E includes detailed classification.

- **Sense features** denote a player’s in-game cognition, reflecting strategic understanding, and tactical anticipation.
  - **Temporal sense features** include temporal features that reflect a player’s gaming sense such as economic considerations, movement dynamics, grenade usage, etc.
  - **Structured sense features** contain structured features that describe in-game understanding, e.g., flash efficiency, prop utilization, etc.
- **Performance features** demonstrate in-game efficacy, indicating engagement capabilities, precision in aiming, and mastery over game mechanisms.
  - **Temporal performance features** include temporal features that indicate continuous in-game performances, e.g., eliminations, damage, weapon proficiency, etc.
  - **Structured performance features** contain the remaining structured features that statistically describe the player’s in-game performances, e.g., elimination-related features.

## V. HAWK

To mimic human experts’ identification process, we propose HAWK which consists of four subsystems: Review Point-of-View (REVPOV), Review Statistics (REVSTATS), Examine Sense-Performance Consistency (EXSPC), and Multi-View Integration (MVIN). The first three subsystems are associated with the three observations we discovered regarding the inherent nature of the cheat identification process in **Section III-A**. MVIN integrates the results derived from the above three subsystems, just as humans integrate the three aspects collectively.

### A. REVPOV

Aligned with **OBS.1**, REVPOV thoroughly examines a player’s time-series operations within a match.

**Multi-LSTM Attention Encoders**: In **Figure 4a**, we feed the seven sets of temporal features (**Section IV-B1**) as input to seven independent Long Short-Term Memory (LSTM) [42] networks to acquire the embeddings. For explanatory purposes, we illustrate the process using the example of the *Economy* features.  $\mathbf{F}_{eco}^n$  denotes the input feature vector. Dropout layers [43] are employed to mitigate the risk of overfitting.  $\vec{h}_G^n$  denotes the output of the encoder, consists of one set of the seven temporal features mentioned in **Section IV-B1**, where  $G$  represents the set and  $n$  indicates the sequence number among all outputs. For each time step, we introduce the Luong-style attention [44] afterward to help the model better understand the importance of different positions in the input sequence and aggregate different parts of the input weights, overcoming the challenge of identifying varying patterns in temporal data for a large number of samples. In **Equation 1**,  $a_G^i$  represents the attention weight for the time step  $i$ .  $\mathbf{W}_q$  and  $\mathbf{W}_k$  denotes the learned weight matrices of *query* and

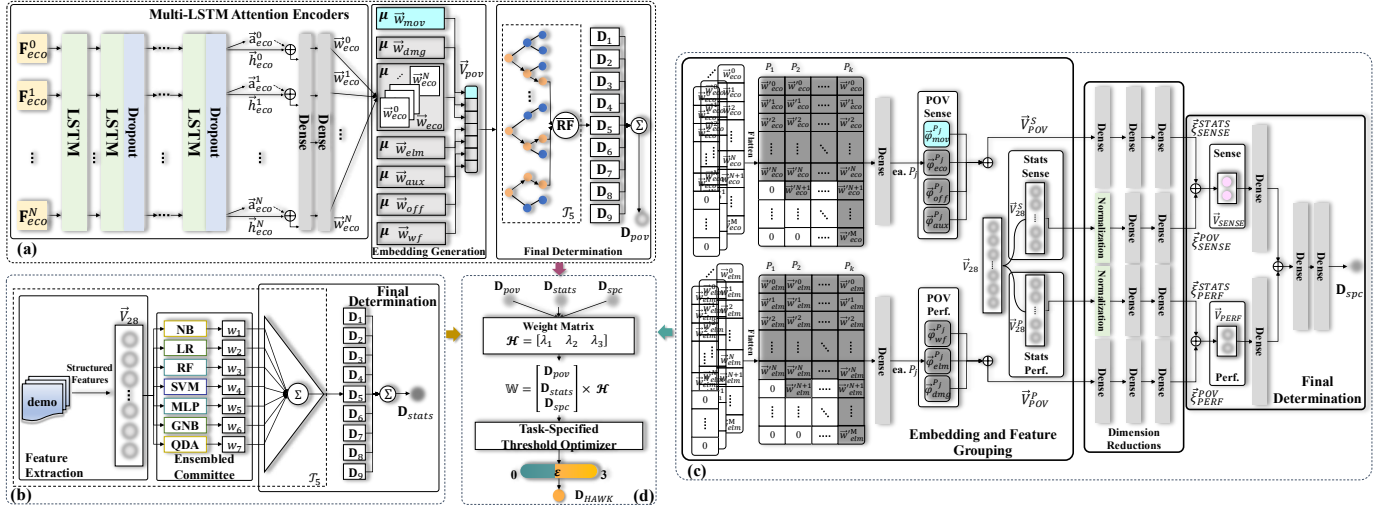


Fig. 4: HAWK framework illustration. (a)-REVPOV, (b)-REVSTATS, (c)-EXSPC are corresponding to three observations in Section III-A, (d)-MVIN is an integration network for combining the determinations from the aforementioned three subsystems.

key in attention mechanism.  $i, j$  and  $k$  indicate different time steps. Concatenation operation is executed afterward, yielding  $[\vec{a}_G^i || \vec{h}_G^i]$ , where  $||$  denotes concatenation. After two dense layers,  $\vec{w}_G^i$  represents the final tensor for binary classification.

$$\vec{a}_G^i = \sum_{j=0}^N \frac{\exp(\mathbf{W}_q \cdot \vec{h}_G^i) \cdot (\mathbf{W}_k \cdot \vec{h}_G^j)}{\sum_{k=0}^N \exp(\mathbf{W}_q \cdot \vec{h}_G^i) \cdot (\mathbf{W}_k \cdot \vec{h}_G^k)} \cdot \vec{h}_G^j \quad (1)$$

**Embedding Generation:** An average pooling in Equation 2 is conducted to flatten the output sequence, where  $N$  denotes the number of output sequences.  $\vec{V}_{pov}$  is the final determination embedding.

$$\vec{w}_G = \frac{\sum_{n=0}^N \vec{w}_G^n}{N+1} \quad (2)$$

$$\vec{V}_{pov} = [\vec{w}_{eco} || \vec{w}_{mov} || \vec{w}_{dmg} || \vec{w}_{elm} || \vec{w}_{aux} || \vec{w}_{off} || \vec{w}_{wf}] \quad (3)$$

**Final Determination:** We find that only depending on the fully connected layers with different activation functions can not effectively classify. Therefore, we conduct the following strategies to further improve REVPOV. In the context of cheat detection, the dataset often exhibits a class imbalance, where the majority of players are honest, inadvertently leading to biased learning towards the dominant class. Therefore, we create a *multi-subsampling* strategy to level the playing field for the minority class, creating balanced representations of both cheating and honest behaviors without dropping any samples. We perform a selective sampling to divide the honest players in the initial training set  $\mathcal{T}$  into nine sets in accordance with the ratio of normal to cheating players, generating nine training sets containing the same set of cheaters and distinct normal players, each denoted as  $\mathcal{T}_k$ , where  $k$  indicates the iteration count. Subsequently, after adding varied examples to the learning process, we obtain nine independent Random Forest models, each corresponding to one of the diversified and balanced training sets  $\mathcal{T}_k$ , we named this strategy as *multi-forest*. The averaging method in Equation 4 is selected for REVPOV final class prediction, where random forest consisting of  $N$  decision trees, each producing a prediction  $h_i(\vec{V}_{pov}^k)$ ,

where  $i$  indicates the  $i$ -th tree,  $k$  denotes the  $k$ -th sampled set, and  $\vec{V}_{pov}^k$  represents the input feature vector.  $p_i$  represents the probability that the  $i$ -th tree predicts sample  $\vec{V}_{pov}^k$  to be in class  $j$ .  $\overline{\mathbf{RF}}(\vec{V}_{pov}^k)$  denotes the average prediction output of the random forest, which is the average of the prediction probability vectors of all decision trees. The prediction for each  $\vec{D}_k$  is obtained by selecting the class with the highest predicted probability shown in Equation 5, where  $(\cdot)_j$  represents the probability of class  $j$  in  $\overline{\mathbf{RF}}(\vec{V}_{pov}^k)$ . After the *multi-forest*, we acquire the corresponding determination  $\mathbf{D}_k$ . Lastly, as in Equation 6, we obtain the final classification determination  $\mathbf{D}_{pov}$  for REVPOV.

$$\overline{\mathbf{RF}}(\vec{V}_{pov}^k) = \frac{1}{N} \sum_{i=1}^N h_i(\vec{V}_{pov}^k) = \frac{1}{N} \sum_{i=1}^N \mathbf{p}_i \quad (4)$$

$$\mathbf{D}_k = \arg \max_j \left( \overline{\mathbf{RF}}(\vec{V}_{pov}^k) \right)_j \quad (5)$$

$$\mathbf{D}_{pov} = \arg \max_j \sum_{k=1}^9 \mathbf{D}_k^{(j)} \quad (6)$$

## B. REVSTATS

Aligned with **OBS.2**, REVSTATS subsystem is designed to perform an in-depth analysis of structured features to capture the cheaters.

**Feature Extraction:** In Figure 4b,  $\vec{V}_{28}$  denotes the vector representation of the structured features (Section IV-A1).

**Ensembled Committee:** During preliminary testing, our selected features showed promising results across most classifiers, demonstrating their effectiveness. However, despite similar performance in terms of metrics alone, the testing revealed that different classifiers produced varying classifications on some individual samples. This suggests that relying on a single classifier, as done in prior works, can lead to unreliable outcomes. However, the majority of classifiers correctly classified the samples, leading to the development of the Ensembled Committee. Among hundreds of classifiers, we identify seven

superior classifiers [45], [46], [47], [48], [49], [50], [51] after the preliminary testing and use them in an ensemble way.

**Final Determination:** Due to imbalanced dataset, a similar *multi-subsampling* strategy as employed in the REVPOV subsystem is adopted for the REVSTATS subsystem to fully leverage the available data without losing valuable information. For each classification model, we generate a distinct model for each subsampled set. Each model is independently trained and provides an individual prediction. A majority voting scheme is utilized within each classification algorithm to aggregate the results of the seven models. The final determination is also achieved through majority voting, which collates the determinations from all nine subsampled sets. In Equation 7, where  $\mathbf{D}_{stats}$  signifies the binary final determination. Where  $w_j$  denotes the decision from the  $j$ th classification algorithm, and  $I(\cdot)$  is the indicator function, returning 1 if the condition within the brackets is true, and 0 otherwise. The decision,  $i$ , which receives the majority of votes from all seven classification algorithms, is accepted as the final determination.

$$\mathbf{D}_{stats} = \arg \max_{i \in \{0,1\}} \sum_{j=1}^7 I(w_j = i) \quad (7)$$

### C. EXSPC

Aligned with **OBS.3**, EXSPC is designed from scratch to inspect the consistency of a player's in-game senses and overall performances.

**Embedding and Feature Grouping:** EXSPC takes seven embeddings and two groups of vectors as input (see **Section IV-C**). The seven embeddings are generated using trained models from REVPOV, while the two vectors are subsets of  $\vec{V}_{28}$  from REVSTATS. Each embedding is padded to the maximum length observed in the dataset. The intermediary result from REVPOV, denoted as  $\vec{w}_G^k$ , represents temporal features, where  $k$  is the sequence number and  $G$  denotes the type of the temporal features. All embeddings are structured as two-dimensional arrays. As illustrated in **Figure 4c**, where  $P_1$  to  $P_k$  represent different players, we exemplify with one player  $P_j$ . The embeddings are first flattened and dimensionally reduced. After processing through seven groups of similar layers, we obtain  $\varphi_G^{P_j}$ . These tensors are then divided into seven types and concatenated for each player. In which,  $\vec{V}_{POV}^S$  denotes the temporal sense features vector and  $\vec{V}_{POV}^P$  denotes the temporal performance features vector. Similarly, the structured features vector  $\vec{V}_{28}$  is divided into two groups: the sense vector  $\vec{V}_{28}^S$  and the performance vector  $\vec{V}_{28}^P$ , as detailed in Supplemental Material E.

**Dimension Reduction:**  $\vec{V}_{28}^S$  and  $\vec{V}_{28}^P$  are normalized. Afterward, each group of the four vectors goes through different groups of dense layers to reduce the dimensions. Next, concatenate four vectors and yield two vectors eventually representing sense  $\vec{V}_{SENSE}$  and performance  $\vec{V}_{PERF}$  respectively.

**Final Determination:** When acquiring  $\vec{V}_{SENSE}$  and  $\vec{V}_{PERF}$ , we further reduce their dimensions and deepen the network for better learning performances. Then, we concatenate two vectors and go through one final dense layer for reducing the dimension and another dense layer with sigmoid activation

function for binary classification. Eventually, the final classification determination  $\mathbf{D}_{spc}$  for EXSPC subsystem is obtained. The class weight is set as one to nine like previous subsystems. Both REVPOV and EXSPC use *Binary Cross-Entropy* as loss function shown in Equation 8, where  $N$  represents the number of samples,  $y_i$  is the true label of the  $i$ -th sample,  $\hat{y}_i$  is the predicted value for the  $i$ -th sample.

$$\text{Loss} = -\frac{1}{N} \sum_{i=1}^N [y_i \log(\hat{y}_i) + (1 - y_i) \log(1 - \hat{y}_i)] \quad (8)$$

### D. MVIN

In **Figure 4d**, MVIN is to dynamically integrate determinations from REVPOV, REVSTATS, and EXSPC.

**Data Integration:** The subsystem integrates the outcomes from REVPOV, REVSTATS, and EXSPC, symbolized as  $\mathbf{D}_{pov}$ ,  $\mathbf{D}_{stats}$ , and  $\mathbf{D}_{spc}$ . Given the diverse nature of these outputs, a structured preprocessing phase becomes indispensable. This step is designed to merge the individual outputs and synchronize them for the succeeding integration process.

**Model Optimization:** MVIN adopts a weight matrix for each subsystem's determination, where weights are dynamically assigned based on the subsystem's importance and reliability. The weighted output,  $\mathbb{W}$ , is calculated as Equation 9. Where  $\lambda_1$ ,  $\lambda_2$ , and  $\lambda_3$  represent the weights associated with the outputs of the subsystems REVPOV, REVSTATS, and EXSPC, respectively.

$$\mathbb{W} = \lambda_1 \cdot \mathbf{D}_{pov} + \lambda_2 \cdot \mathbf{D}_{stats} + \lambda_3 \cdot \mathbf{D}_{spc} \quad (9)$$

**Final Determination:**  $\mathbb{W}$  undergoes a learnable thresholding via the *Task-Specified Threshold Optimizer* (TSTO), which provides a binary determination based on a dynamic threshold  $\varepsilon$ . The threshold optimizer can be dynamically set based on anti-cheat requirements. For instance, in *Recall* mode, the optimizer would aim to identify every potential cheater, accepting the risk of higher false positives. This threshold  $\varepsilon$  therefore acts as a decision boundary, converting the continuous weighted value  $\mathbb{W}$  into a discrete binary outcome  $\mathbf{D}_{HAWK}$ . TSTO offers HAWK a degree of selectivity, enabling flexible tuning and offering promising performance without requiring retraining any prior subsystems, overcoming the challenge of lack of system adaptability. By harnessing the strengths of each subsystem and compensating for their limitations, MVIN is crucial to integrate determinations from different subsystems.

## VI. EXPERIMENTS

We conduct experiments to answer seven research questions (**RQ.1–RQ.7**):

- **RQ.1:** What are the performances of HAWK and each subsystem? (**Section VI-C**)
- **RQ.2:** To what extent has HAWK improved effectiveness and efficiency compared to current official inspections? (**Section VI-D**)
- **RQ.3:** What are the performances of HAWK under different settings of the *Task-Specified Threshold Optimizer*? (**Section VI-F**)
- **RQ.4:** What is the robustness of HAWK and its subsystems against cheat evolution? (**Section VI-G**)

- **RQ.5:** Is there any suspicious activity that still exists but has never been detected by officials? (Section VI-H)
- **RQ.6:** What is the overhead of HAWK? (Section VI-I)
- **RQ.7:** Is HAWK performing better than prior works? (Section VI-E)



Fig. 5: Experiments' process and labeling details.

TABLE II: Dataset separation and description.

CT <sup>1</sup>	Train				Validation				Test			
	#M <sup>2</sup>	#P <sup>3</sup>	#N <sup>4</sup>	#C <sup>5</sup>	#M	#P	#N	#C	#M	#P	#N	#C
Aimbot	1,009	10,127	9,150	977	975	8,561	7,697	864	995	9,047	8,163	884
Wallhack	833	8,320	7,500	820	1,037	9,712	8,745	967	1,101	10,274	9,249	1,025

<sup>1</sup>CT: Cheat type; <sup>2</sup>#M: Number of matches; <sup>3</sup>#P: Number of players in total; <sup>4</sup>#N: Number of normal (honest) players; <sup>5</sup>#C: Number of cheaters.

### A. Incomparability to Prior Works

First, most prior works are not open-sourced as listed in Table I. Second, the data collection method is incompatible. HAWK relies on post-game *replay files*, whereas prior studies modified the game engine or applied mods during gameplay. Prior works are unable to extract data from the *replay files*. Third, installation on commercial clients or servers is infeasible. Only if the prior designs are implemented before the data collection, the data can then be gathered and evaluated. However, the partner platform prohibits installing unverified programs on clients or servers due to legal restrictions. In addition to the aforementioned reasons with commonality, we also further state below the specific reasons for the detailed incomparability between HAWK and the SOTA designs. There are three aspects of incomparability with BotScreen [6]. First, BotScreen's data extraction is highly coupled with the game version and deprecated. The authors of BotScreen confirmed through email that their data extraction does not apply to the current game versions. Second, the deprecation of Intel SGX [14], [15] prevents us from conducting comparative experiments. Third, it can only detect *pure aimbot*, making the comparison less significant. Invisibility Cloak [8] and BlackMirror [9] are prevention designs only for counteracting *computer-vision-based aimbots* and *wallhacks*, respectively. Both studies are only functional before the cheats happen.

Whereas HAWK and other prior works are detection systems that function after cheating. We detailed the incomparability to prior works in Table III. We manage to compare HAWK

<sup>3</sup>Commercial anti-cheat (detailed in Section VIII), not open-source, leverages reverse engineering on the known cheats to detect cheating signatures.

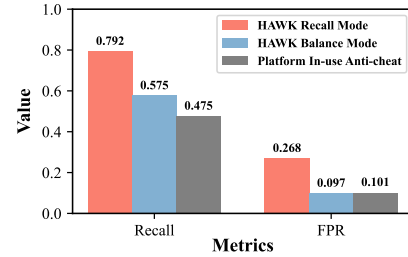


Fig. 6: Recall and FPR performance comparison among HAWK-Recall priority mode, HAWK-Balance mode, and our partner in-use anti-cheat<sup>3</sup>. HAWK's different modes are introduced and evaluated in Section V-D and Section VI-F.

with our partner's industrial in-use anti-cheat in Figure 6 and reproduce two server-side works [11], [12] for further comparison in Table IX.

### B. Experimental Settings and Ground Truth

The *demos* are open-sourced and acquired from a well-known CS:GO platform<sup>4</sup>. The initial data extraction utilizes a public library *awpy* [52] to parse the *demo* into a JSON file, which contains the raw data for HAWK's feature constructions.

Table II is the dataset description. Figure 5 illustrates our experimental process. We evaluate HAWK with two of the most prevalent cheat types, *aimbot* and *wallhack*. For *aimbot*, data is collected over a single 16-day window, while for *wallhack*, two collection windows totaling 27 days are used (the rationale for this inconsistency is explained in Section VI-G). All *demos* are from real-world ranked matches within these windows, ensuring that the cheats used by players remain black-box to the anti-cheat system. Both datasets naturally contain varying levels of cheating sophistication. The cheaters' labels in the *first labeling* are acquired on the last day of data collection for each set. These labels are used for training and most evaluations, as illustrated in Figure 5. Official inspections, which include proprietary closed-source anti-cheat systems and manual checks, are conducted continuously, with daily updates to the ban list. However, due to the lengthy ban cycle, most cheaters are not banned immediately after cheating. To address this, a *second labeling* is performed 65 days after the *first labeling* to identify cheaters who were initially mislabeled. This allowed us to refine our analysis of false positives, with the updated cheater counts detailed in Table VI.

Official inspections employ a combination of proprietary anti-cheat software, developed by *5Eplay*, and manual verification. The anti-cheat system operates by installing a kernel-level driver to scan system memory and active processes for known cheat signatures. A significant drawback of this method is its inherent reliance on a blacklist, making it one step behind the cheating developers. Modern cheats frequently update their code and employ advanced obfuscation techniques to evade signature-based detection. When a potential violation is identified, the system forwards the detection results to human reviewers for final determination. Note that despite

<sup>4</sup>5EPlay: <https://www.5eplay.com/>.

TABLE III: Incomparability to prior works.

Work	Task		Data Extraction				Targeting		Hardware Constraint	Code Availability
	Detection	Prevention	Runtime	Replay file	Aimbot	Wallhack				
BotScreen [6]	✓		✓ (deprecated)				✓		Intel SGX (deprecated)	✓
BlackMirror [9]		✓	✓					✓	Intel SGX (deprecated)	✓
Invisibility Cloak [8]		✓	✓				✓		None	✓
Prior works [10], [11], [12], [13]	✓		✓ (unavailable)				✓		None	✗
HAWK	✓			✓			✓	✓	None	✓

TABLE IV: Ablation study results on each of the subsystems.

CT	System	Validation									Test								
		TP	TN	FP	FN	Accuracy	Recall	NPV	AUC-ROC	FPR	TP	TN	FP	FN	Accuracy	Recall	NPV	AUC-ROC	FPR
Aimbot	REVPOV	458	4,796	2,901	406	0.614	0.530	0.922	0.577	0.378	481	5,088	3,075	403	0.616	0.544	0.927	0.584	0.377
	REVSTATS	453	7,290	407	411	0.904	0.524	0.947	0.736	0.053	566	6,797	1,366	318	0.814	0.640	0.955	0.736	0.167
	ExSPC	553	6,187	1,510	311	0.787	0.640	0.952	0.779	0.196	558	6,616	1,547	326	0.793	0.631	0.953	0.786	0.190
	REVPOV+REVSTATS	648	4,603	3,094	216	0.613	0.750	0.955	0.760	0.402	691	4,364	3,799	193	0.559	0.782	0.958	0.750	0.465
	REVPOV+ExSPC	611	5,733	1,964	253	0.741	0.707	0.958	0.781	0.255	608	6,082	2,081	276	0.739	0.688	0.957	0.784	0.255
	REVSTATS+ExSPC	605	5,828	1,869	259	0.751	0.700	0.957	0.798	0.243	639	5,877	2,286	245	0.720	0.723	0.960	0.796	0.280
	HAWK	614	5,803	1,894	250	0.750	0.711	0.959	0.732	0.246	642	5,837	2,326	242	0.716	0.726	0.960	0.721	0.285
Wallhack	REVPOV	573	6,081	2,664	394	0.685	0.593	0.939	0.644	0.305	627	6,364	2,885	398	0.680	0.612	0.941	0.650	0.312
	REVSTATS	604	8,241	504	363	0.911	0.625	0.958	0.783	0.058	855	6,988	2,261	170	0.763	0.834	0.976	0.795	0.245
	ExSPC	760	7,258	1,487	207	0.826	0.786	0.972	0.885	0.170	501	8,484	765	524	0.875	0.489	0.942	0.840	0.083
	REVPOV+REVSTATS	604	8,241	504	363	0.911	0.625	0.958	0.798	0.058	855	6,988	2,261	170	0.763	0.834	0.976	0.816	0.244
	REVPOV+ExSPC	806	6,900	1,845	161	0.793	0.834	0.977	0.885	0.211	573	8,257	992	452	0.859	0.559	0.948	0.840	0.107
	REVSTATS+ExSPC	791	7,110	1,635	176	0.814	0.818	0.976	0.889	0.187	868	6,907	2,342	157	0.757	0.847	0.978	0.859	0.253
	HAWK	798	7,033	1,712	169	0.806	0.825	0.977	0.815	0.196	869	6,902	2,347	156	0.756	0.848	0.978	0.797	0.254

TABLE V: Selected comparison result between different superior baseline models and REVSTATS.

CT	Model	Validation									Test								
		TP	TN	FP	FN	Accuracy	Recall	NPV	AUC-ROC	FPR	TP	TN	FP	FN	Accuracy	Recall	NPV	AUC-ROC	FPR
Aimbot	LogisticRegression [46]	570	6,204	1,493	294	0.791	0.660	0.955	0.733	0.194	713	4,897	3,266	171	0.620	0.807	0.966	0.703	0.400
	Naive Bayes [49]	467	6,740	957	397	0.842	0.874	0.944	0.708	0.124	625	5,928	2,235	259	0.724	0.707	0.958	0.717	0.274
	RandomForest [47]	415	7,694	3	449	0.947	0.480	0.945	0.740	0.000	427	7,634	529	457	0.891	0.483	0.944	0.709	0.065
	SVM [48]	309	7,615	82	555	0.926	0.358	0.932	0.673	0.011	405	7,665	498	479	0.892	0.458	0.941	0.699	0.061
	MLP [45]	858	7,697	0	6	0.999	0.993	0.999	0.997	0.000	508	7,325	838	376	0.866	0.575	0.951	0.736	0.103
	GaussianNB [50]	467	6,740	957	397	0.842	0.541	0.944	0.708	0.124	625	5,928	2,235	259	0.724	0.707	0.958	0.717	0.274
	QDA [51]	350	7,181	516	514	0.880	0.405	0.933	0.669	0.067	534	6,770	1,393	350	0.807	0.604	0.951	0.717	0.171
	REVSTATS	453	7,290	407	411	0.904	0.524	0.947	0.736	0.053	566	6,797	1,366	318	0.814	0.640	0.955	0.736	0.167
		HAWK	614	5,803	1,894	250	0.750	0.711	0.959	0.732	0.246	642	5,837	2,326	242	0.716	0.726	0.960	0.721
Wallhack	LogisticRegression	714	7,629	1,116	253	0.859	0.738	0.968	0.805	0.128	943	5,622	3,627	82	0.639	0.920	0.986	0.764	0.392
	Naive Bayes	604	7,677	1,068	363	0.853	0.625	0.955	0.751	0.122	891	6,103	3,146	134	0.681	0.869	0.979	0.765	0.340
	RandomForest	967	8,745	0	0	1.000	1.000	1.000	1.000	0.000	751	8,083	1,166	274	0.860	0.733	0.967	0.803	0.126
	SVM	548	8,323	422	419	0.913	0.567	0.952	0.759	0.048	817	7,227	2,022	208	0.783	0.797	0.972	0.789	0.219
	MLP	472	8,489	256	495	0.923	0.488	0.945	0.729	0.029	788	7,726	1,523	237	0.829	0.769	0.970	0.802	0.165
	GaussianNB	604	7,677	1,068	363	0.853	0.625	0.955	0.751	0.122	891	6,103	3,146	134	0.681	0.869	0.979	0.765	0.340
	QDA	493	8,276	469	474	0.903	0.510	0.946	0.728	0.054	815	7,270	1,979	210	0.787	0.795	0.972	0.791	0.214
	REVSTATS	604	8,241	504	363	0.911	0.625	0.958	0.783	0.058	855	6,988	2,261	170	0.763	0.834	0.976	0.795	0.245
		HAWK	798	7,033	1,712	169	0.806	0.825	0.977	0.815	0.196	869	6,902	2,347	156	0.756	0.848	0.978	0.797

5EPlay tried their best to annotate the samples as accurately as possible. This process inherently and inevitably introduces a small amount of false negatives (i.e., the cheaters who escape the inspections) after the *second labeling* due to the current limitation of anti-cheat low performance. This is an unsolvable dilemma for this area. All positive samples (cheaters) are accurately labeled.

The increase of cheaters between the first and second labeling is indicated in Table VI’s *#IncrPs*. Based on 5EPlay’s statistics and the case study in Section VI-H, there are approximately 1.5%-2% and 3%-4% uncaught cheaters in the negative samples after the *second labeling* across different sets in the *Aimbot* and *Wallhack* datasets, respectively.

Although the two datasets include different cheat types, the official in-use anti-cheat systems cannot label specific subcategories; they only annotate broad cheat categories. Quantifying cheating sophistication is inherently subjective and challenging, making it infeasible to provide a more detailed breakdown of the datasets. Additionally, due to the poor performance of current anti-cheat systems, the ground truth inevitably contains noise (cheaters who evade detection) within the negative labels. But to the best of our knowledge, this is the most realistic and well-annotated dataset.

To evaluate how effectively cheaters are identified, we use the metrics, accuracy, recall, NPV, AUC-ROC, and FPR, defined in Supplemental Material G.

TABLE VI: The manual average ban duration comparison and the remediation rate among HAWK’s false positives after the first labeling.

CT	HAWK <sup>1</sup>	Off. <sup>2</sup>	Validation			Test		
			#MTPs <sup>3</sup>	Rmd% <sup>4</sup>	#IncrPs <sup>5</sup>	#MTPs	Rmd%	#IncrPs
Aimbot	~4 min	5.88 days	93	4.91%	237	97	4.17%	233
Wallhack		4.47 days	93	5.43%	226	153	6.52%	303

<sup>1</sup>HAWK: The process time of HAWK varies with match length, HAWK’s detailed overheads are evaluated in Section VI-I; <sup>2</sup>Off.: The average ban duration of official manual inspections per match; <sup>3</sup>#MTPs: The number of missed true positives among the false positives; <sup>4</sup>Rmd%: The percentage of #MTPs in the number of false positives; <sup>5</sup>#IncrPs: The number of increased positives (cheaters) labeled by the officials after the second labeling.

### C. Overall Performance, Ablation and Baseline Comparison

To answer RQ.1, we conduct an ablation study, shown in Table IV. We set the TSTO to achieve the highest accuracy with at least 70% recall for detecting *aimbot*, and the highest AUC-ROC for detecting *wallhack* (same below unless otherwise stated), illustrating different anti-cheat scenarios

TABLE VII: Comparison result on the different baseline models of REVPOV.

CT	Model	Validation								Test									
		TP	TN	FP	FN	Accuracy	Recall	NPV	AUC-ROC	FPR	TP	TN	FP	FN	Accuracy	Recall	NPV	AUC-ROC	FPR
Aimbot	REPTree [53]	19	7,660	37	845	0.897	0.022	0.901	0.509	0.005	33	8,118	45	851	0.901	0.037	0.905	0.516	0.006
	RandomTree	123	6,914	783	741	0.822	0.142	0.903	0.520	0.102	125	7,399	764	759	0.832	0.141	0.907	0.524	0.094
	RseslibKNN [54]	40	7,460	237	824	0.876	0.046	0.901	0.508	0.031	33	7,868	295	851	0.873	0.037	0.902	0.501	0.036
	SPAARC [55]	0	7,697	0	864	0.899	0.000	0.899	0.500	0.000	0	8,163	0	884	0.902	0.000	0.902	0.500	0.000
	RandomForest [47]	16	7,665	32	848	0.897	0.019	0.900	0.507	0.004	33	8,128	35	851	0.902	0.037	0.905	0.517	0.004
	Bagging [56]	18	7,666	31	846	0.898	0.021	0.901	0.508	0.004	30	8,129	34	854	0.902	0.034	0.905	0.515	0.004
	VFI [57]	822	445	7,252	42	0.148	0.951	0.914	0.505	0.942	848	472	7,691	36	0.146	0.959	0.929	0.509	0.942
	JRip [58]	21	7,663	34	843	0.898	0.024	0.901	0.510	0.004	42	8,116	47	842	0.902	0.048	0.906	0.521	0.006
	MODLEM [59]	19	7,588	109	845	0.889	0.022	0.900	0.504	0.014	34	8,029	134	850	0.891	0.038	0.904	0.511	0.016
	CSForest [60]	50	7,292	405	814	0.858	0.058	0.900	0.503	0.053	58	7,755	408	826	0.864	0.066	0.904	0.508	0.050
REVPOV	458	4,796	2,901	406	0.614	0.530	0.922	0.577	0.377	481	5,088	3,075	403	0.616	0.544	0.927	0.584	0.377	
Wallhack	REPTree	47	8,641	104	920	0.895	0.049	0.904	0.518	0.012	66	9,140	109	959	0.896	0.064	0.905	0.526	0.012
	RandomTree	178	8,006	738	789	0.843	0.184	0.910	0.550	0.084	198	8,433	816	827	0.840	0.193	0.911	0.552	0.088
	RseslibKNN	89	8,515	230	878	0.886	0.092	0.907	0.533	0.026	120	8,939	310	905	0.882	0.117	0.908	0.542	0.034
	SPAARC	69	8,679	66	898	0.901	0.071	0.906	0.532	0.008	87	9,164	85	938	0.900	0.085	0.907	0.538	0.009
	RandomForest	27	8,713	32	940	0.900	0.028	0.903	0.512	0.004	35	9,212	37	990	0.900	0.034	0.903	0.515	0.004
	Bagging	26	8,705	40	941	0.899	0.027	0.902	0.511	0.005	37	9,201	48	988	0.899	0.036	0.903	0.515	0.005
	VFI	950	563	8,182	17	0.156	0.982	0.971	0.523	0.936	1,008	689	8,560	17	0.166	0.983	0.976	0.529	0.925
	JRip	36	8,670	75	931	0.896	0.037	0.903	0.514	0.009	71	9,179	70	954	0.900	0.069	0.906	0.531	0.008
	MODLEM	35	8,687	58	932	0.898	0.036	0.903	0.515	0.007	56	9,171	78	969	0.898	0.055	0.904	0.523	0.008
	CSForest	0	8,745	0	967	0.900	0.000	0.900	0.500	0.000	0	9,249	0	1,025	0.900	0.000	0.900	0.500	0.000
REVPOV	573	6,081	2,664	394	0.685	0.593	0.939	0.644	0.305	627	6,364	2,885	398	0.680	0.612	0.941	0.650	0.312	

TABLE VIII: HAWK detection result with different *Task-Specified Threshold Optimizer (TSTO)* settings.

CT	TSTO	Validation								Test									
		TP	TN	FP	FN	Accuracy	Recall	AUC-ROC	NPV	FPR	TP	TN	FP	FN	Accuracy	Recall	AUC-ROC	NPV	FPR
Aimbot	Balance <sup>1</sup>	389	7,390	307	475	0.909	0.450	0.705	0.940	0.040	457	7,444	719	427	0.873	0.517	0.714	0.946	0.088
	F1-Score	448	7,305	392	416	0.906	0.519	0.734	0.946	0.051	548	6,928	1,235	336	0.826	0.620	0.734	0.954	0.151
	Accuracy	269	7,528	169	595	0.911	0.311	0.645	0.927	0.022	305	7,888	275	579	0.906	0.345	0.656	0.932	0.034
	AUC-ROC	648	4,603	3,094	216	0.613	0.750	0.674	0.955	0.402	691	4,364	3,799	193	0.559	0.782	0.658	0.958	0.465
	$Acc_{rc>0.75}$ <sup>2</sup>	652	5,321	2,376	212	0.698	0.755	0.723	0.962	0.309	672	5,365	2,798	212	0.667	0.760	0.709	0.962	0.343
	$Acc_{rc>0.8}$	700	4,611	3,086	164	0.620	0.810	0.705	0.966	0.401	716	4,700	3,463	168	0.599	0.810	0.693	0.965	0.424
	$Acc_{rc>0.85}$	736	3,790	3,907	128	0.529	0.852	0.672	0.967	0.508	761	3,875	4,288	123	0.512	0.861	0.668	0.969	0.525
$Acc_{rc>0.9}$	778	2,859	4,838	86	0.425	0.900	0.636	0.971	0.628	787	2,955	5,208	97	0.414	0.890	0.626	0.968	0.638	
Wallhack	Balance	592	8,256	489	375	0.911	0.612	0.778	0.957	0.056	616	8,344	905	409	0.872	0.601	0.752	0.953	0.098
	F1-Score	576	8,313	432	391	0.915	0.596	0.773	0.955	0.049	651	8,040	1,209	374	0.846	0.635	0.752	0.956	0.131
	Accuracy	374	8,582	163	593	0.922	0.387	0.684	0.935	0.019	167	9,158	91	858	0.908	0.163	0.577	0.914	0.010
	$Acc_{rc>0.7}$	677	7,898	847	290	0.883	0.700	0.802	0.965	0.097	803	7,506	1,743	222	0.809	0.783	0.797	0.971	1.188
	$Acc_{rc>0.75}$	727	7,589	1,156	240	0.856	0.752	0.810	0.969	0.132	859	6,964	2,285	166	0.761	0.838	0.795	0.977	0.247
	$Acc_{rc>0.8}$	776	7,186	1,559	191	0.820	0.802	0.812	0.974	0.178	583	8,280	969	442	0.863	0.569	0.732	0.949	0.105
	$Acc_{rc>0.85}$	822	6,712	2,033	145	0.776	0.850	0.809	0.979	0.232	871	6,810	2,439	154	0.748	0.850	0.793	0.978	0.264
$Acc_{rc>0.9}$	871	5,755	2,990	96	0.682	0.901	0.779	0.984	0.342	855	6,885	2,364	170	0.753	0.834	0.789	0.976	0.256	

<sup>1</sup>Balance: maintain industry-standard FPR (shown in Figure 6) while optimizing recall; <sup>2</sup> $Acc_{rc>n}$ : highest accuracy while maintaining recall above  $n$ .

(further evaluated in Section VI-F). Overall, HAWK excels in identifying authentic cheaters, evidenced by the highest *recall* and *NPV* across all evaluations. For *aimbot* detection, REVSTATS enhances *accuracy* by effectively filtering normal players in both validation and test sets. In *wallhack* detection, REVSTATS excels in the validation set, while EXSPC leads in the test set. Although some components like REVSTATS and EXSPC outperform HAWK in *accuracy* and *FPR*, their lower *recall* (up to 64%) limits their effectiveness, affirming HAWK as the optimal choice. Notably, the *Wallhack* dataset yields better overall performance than *Aimbot*. We believe this is due to the latter's diverse subcategories of *aimbots*. We conduct the pair-wise ablation study to evaluate the performance among HAWK and different combinations of subsystems. In Table IV, we observe that REVPOV and REVSTATS combination has significantly higher *FPR* on the *Aimbot* set and slightly lower *recall* on the *Wallhack* set. The other two combinations both suffer from lower *recall*. While evaluating the performance, we prioritize *recall*, *accuracy* and *FPR* on the test set over other metrics, because they can more directly reflect the ability to identify cheaters or the overall performance. HAWK's framework is designed with both detection effectiveness and efficiency in mind. We select models with acceptable detection performance, and further select models with low training and prediction costs based on the overhead described in the relevant articles. Table VII and Table V show REVPOV's and

REVSTATS's promising model selection results among hundreds of tested baselines. REVPOV outperforms other models with balanced, consistent accuracy and recall. For REVSTATS, we found that Random Forest outperformed other models. Yet, it sometimes failed to overcome the overfitting problem (e.g., wallhack validation set). Thus, we adopt *multi-forest* and *multi-subsampling* with Random Forest. As a result, REVSTATS outperforms individual classifiers in balancing recall and accuracy by capitalizing on the strengths of each classifier. We also prioritize metrics *recall*, *accuracy* and *FPR* on the test set over other metrics. For example, although Logistic Regression has a higher *recall*, its *accuracy* and *FPR* are significantly lower. The contribution of the *recall*'s increase can not make up for the decrease in accuracy and *FPR*.

The current framework has optimized overall performance compared with more innovative models. For example, in the preliminary test of REVPOV's encoder selection, we obtain lower detection performance with extended training and testing time while using the Transformer.

#### D. HAWK and Official Inspection Comparison

To answer RQ.2, we calculate the daily number of bans for the day and cumulative ban-sums by HAWK and the official inspections illustrated in Figure 7. The figure indicates that HAWK's identification effectiveness (daily count in red bars) and efficiency (cumulative count in solid red lines) outrank

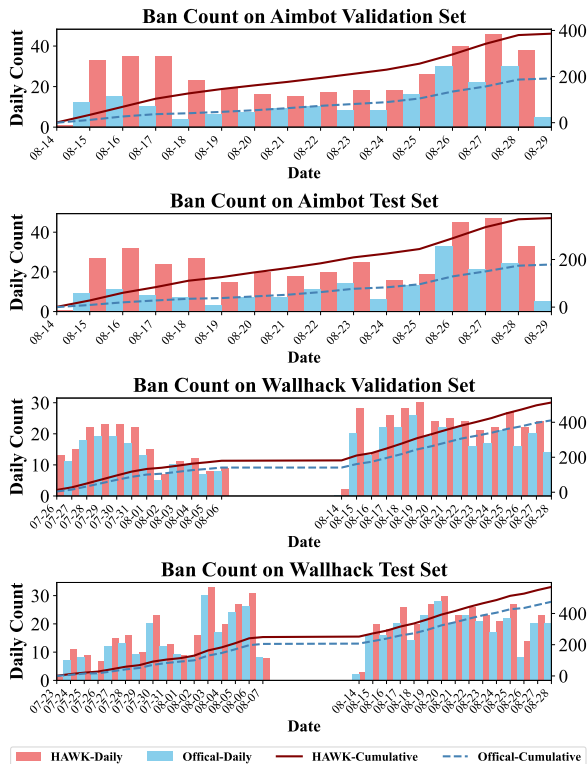


Fig. 7: Daily number of bans for the day and cumulative bans by HAWK versus the official manual inspections.

those of the official manual inspections (hatched blue bars and dashed blue lines) on both cheat types. Additionally, Table VI compares the average ban duration per match, revealing that HAWK’s seconds-scale processing time is exponentially more efficient than official inspections. The remediation rate indicates the percentage of cheaters not banned in the first labeling but caught in the second labeling. Table VI lists the remediation rate after the second labeling among HAWK’s false positives (which are obtained after the first labeling). It demonstrates that HAWK can capture the authentic cheaters who escape from the official anti-cheat system. Moreover, this indicates that HAWK is robust against mislabeled data. We also compare the HAWK’s performance with the official in-use anti-cheat in the next section, as it is relevant to MVIN.

TABLE IX: HAWK comparative study results to prior works on the *Aimbot* test set. The optimal results are bolded.

Method	Accuracy	Recall	NPV	AUC-ROC	FPR
AccA[11]	0.103	<b>0.997</b>	0.897	0.558	0.997
HitAcc[12]	0.675	0.545	0.931	0.658	0.311
<b>HAWK</b>	<b>0.716</b>	0.726	<b>0.960</b>	<b>0.721</b>	<b>0.285</b>

### E. Comparative Analysis Among HAWK and Prior Works

To answer RQ.7, we compare HAWK with two other reproduced methods using HAWK’s *Aimbot* dataset. Due to the lack of available open-source solutions, we write our own code to reproduce both *aimbot* detection methods based on statistical

features related to aiming or elimination used in prior works. Both methods are related to HAWK but use naive statistical features, data, and approach. Since prior work only targeted *aimbots*, we only used the *Aimbot* dataset for comparison. The results are listed in Table IX. HAWK outperforms prior works across all metrics but ACCA’s recall, because ACCA classifies most of the samples as cheaters. Below is a summary of each method:

- ACCA: Filters cheaters when the player’s field-of-view acceleration exceeds a threshold [11].
- HITACC: Filters cheaters based on the weapon accuracy of the player, using SVM [12].

### F. Analysis on Different MVIN Settings

To address RQ.3, we conduct a comparative analysis of HAWK under different MVIN settings, as shown in Table VIII and Figure 6. In Table VIII, except MVIN, other subsystems are trained and validated with recall priority. By only adjusting the TSTO in MVIN, HAWK achieves rapid dynamic tuning ability, by using pre-trained MVIN or retraining MVIN to generate weight matrices and thresholds in about one minute. For example, the TSTO settings can be adjusted to achieve a lower FPR if necessary, avoiding the potential surge of excessive manual verification workload. Table VIII shows that leveraging different optimizer settings, e.g., *Accuracy* or *F1-Score* optimization modes, can obtain low FPR (1%-3% or 5%-15%, respectively). Alternatively, the *Balance* mode maintains a lower FPR than current industry standards (grey bar in Figure 6) while optimizing recall, resulting in slightly lower FPR and significantly higher recall compared to industry anti-cheat system (see blue bars in Figure 6, industry anti-cheats are introduced in Section VIII).

### G. Robustness to Cheat Evolution

Although anti-cheat measures are often opaque to prevent circumvention, cheat developers treat them as black boxes, adapting and camouflaging their cheats on a timely basis to evade detection. *Cheat evolution* refers to the diminishing effectiveness of specific anti-cheat over time. Commercially used anti-cheat methods are susceptible to this evolution (explained in Section VIII). However, HAWK starts the analysis from the behavior, thus cheaters must appear the data-level distinctions mentioned in Section II-B. Hence, no matter how the cheats adapt, as long as the cheaters still want to gain unfair advantages, it is hard to bypass the detection of HAWK. To address RQ.4, we test HAWK’s robustness to cheat evolution using the *Aimbot* dataset. Classified through date, the dataset is divided into partitions (40 *matches* per partition). The training and validation are performed on all data up to the current partition. We compared its performance on the same test set with different partitions’ trained models. The reason for selecting the *Aimbot* dataset is that during its collection window, an official mass ban on *aimbots* took place (at the 10th partition), and the cheats are usually updated within a few days after such an incident. Figure 8a and Figure 8b demonstrate the ablated performances of subsets under different metrics of

HAWK across different numbers of partitions for training. According to the average ban duration of the official bans in Table VI, approximately three sequestration ban cycles have passed during the collection window, and at least two ban cycles after the mass ban occurred. This offers more than enough time for cheat to evolve. The ablated results of HAWK on both sets have been fluctuating to maintain within a small range over partitions (time) and with the cheat evolution. This indicates even without using the latter models of partitioned samples after the mass ban, HAWK's performance remains stable on the test set before and after the mass ban occurred. Besides, in Figure 7, we observe the effectiveness of HAWK has not continuously decreased over time on both datasets (we separated and extended the collection windows in *Wallhack* dataset for further proof). Thus, both experiments indicate HAWK is robust to cheat evolution.

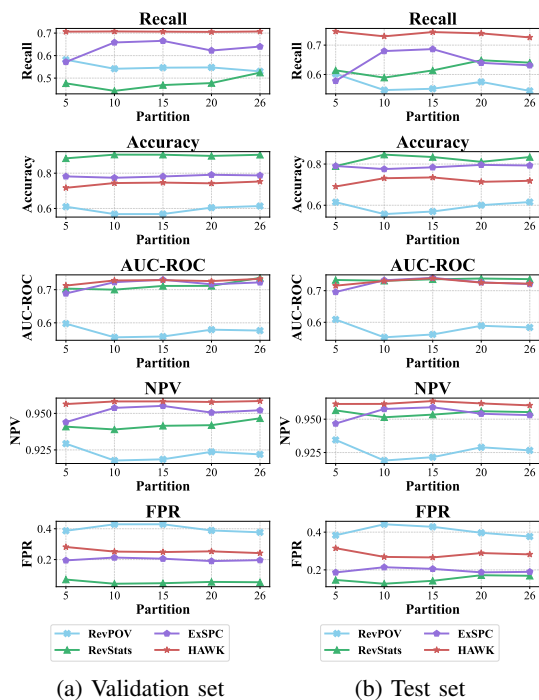


Fig. 8: Ablated robustness against cheat evolution under different metrics for validation (a) and test (b) sets.

#### H. Detecting Uncaught Cheaters in the Wild

To answer RQ.5, given the above-known presence of cheaters in the false positives in Table VI after the *first labeling*, we conduct a use case analysis to explore if there are additional illegal activities that exist after the *second labeling*. Given the lengthy average duration of a match, which demands significant manpower, we select the top 30 HAWK's false positives based on the decreasing order of the *akpr* from the *Aimbot* and *Wallhack* validation sets for manual review, respectively (experts' skill level is listed in Supplemental Material Table 1). With the assistance of three experts in FPS games, we identify 27 suspects, who are labeled as *normal players* after the second labeling, to be highly suspicious within these 60 false positives. Of these 27 suspects, 14 originate from the *Aimbot* dataset (4 are considered using *aimbots*

and 10 are considered *boosting*, i.e., elevate the account rank by other higher-rank players playing the account), while 13 are from the *Wallhack* dataset (8 are considered using *wallhacks* and 5 are considered *boosting*). We reported these suspicions to the official personnel. Upon their review, they confirm all 12 of the aforementioned *aimbots* and *wallhacks* suspects are committed to cheats, subsequently issuing bans for these cheaters. This reaffirms the poor performance of current in-use anti-cheats. The website mentioned in Section I demonstrates their illegal actions. In terms of *boosting* suspects, there are no existing solutions for the officials to evidently verify their illegal actions. Therefore, there are no bans issued on the suspicious *boosting* accounts. This experiment further proves the limited performance of current industrial anti-cheats, while demonstrating HAWK's superior anti-cheat capabilities and high robustness to noise.

#### I. Overheads

HAWK is designed as an asynchronous, load-balancing system that analyzes post-game *replay files* during periods of low server activity. It operates independently of active game servers and can be deployed on a separate server. However, we still conduct overhead assessments for reference. To answer RQ.6, we utilize an Ubuntu server equipped with 128 cores AMD EPYC 7713P 64-Core Processor and 256 GB RAM, a real dedicated game server configuration [61]. Leveraging the pre-trained model in the artifact, HAWK requires only CPU resources to function efficiently. Table X shows the maximum overhead statistics per match, with each match analyzed concurrently. Additionally, we estimate the HAWK-to-server overheads in terms of a real deployment scenario. Our partner platform reports that at most 150,000 matches are played daily, with each server needing to handle up to 573 matches a day. According to our platform's report and public server statistics [62], player activity is lowest between 1-5 AM local time, requiring analysis of up to 144 matches per hour. Based on the elapsed time in Table X, HAWK needs to process up to 12 matches concurrently to complete all analyses within the timeframe per server. We further conduct concurrent processing evaluation, it occupies at most 17.95% memory and 35.45% CPU usage for processing 12 matches concurrently. Therefore, each server has more than sufficient resources for deploying HAWK, even when hosting several matches simultaneously. It is vital for a design to maintain stable performance in high-concurrency environments [63]. To further validate the performance of HAWK under varying concurrency levels, we employed a game server equipped with a 24-core Intel® Xeon® Gold 5418Y CPUs and 503 GB RAM. During idle periods on this server, we concurrently request HAWK 10, 20, and 50 times, respectively. The results are listed in Table XI. The system maintains stable performance when handling different levels of concurrent requests. Furthermore, based on the aforementioned server load data, each server requires running HAWK concurrently 12 times per hour at most. Our tests reached a maximum concurrency of 50 requests, exceeding the data upper bound by over four times. But HAWK requires less than 7 minutes

to complete all 50 requests. Therefore, we conclude that using HAWK under high concurrency conditions does not significantly affect the system overhead.

TABLE X: Maximum overheads of HAWK’s subsystems per match. The numbers are retrieved by the Time [64] in Linux.

Max. Overheads per Match	REVPOV	REVSTATS	EXSPC	MVIN
User time (sec)	415.72	178.12	36.89	3.97
System time (sec)	69.32	436.61	27.12	13.53
Elapsed time (mm:ss)	03:40	00:14	00:45	00:01
Percent of CPU this job got	220%	4371%	140%	2860%
Maximum resident set size (GB)	3.56	0.27	2.57	0.10

TABLE XI: Performance under varying concurrency levels.

# Concurrent Request	10	20	50
Average time (sec)	384.512	365.267	377.084
Minimum time (sec)	380.343	357.570	368.070
Maximum time (sec)	393.472	391.536	386.522
Standard deviation	4.502	7.793	5.282

## VII. DISCUSSIONS

**Generalizability.** Narrowed generalizability is a meta-problem in the anti-cheat field. Since cheats are game-specific, creating a universal anti-cheat system is challenging. Although we successfully implemented HAWK on a leading tactical shooter game [65] (a subgenre of FPS games like CS:GO), similar to prior works [6], [10], [11], [12], [13] discussed in Section VIII, it requires further adaptation for other FPS subgenres with distinct gameplay. The proposed features are applicable to tactical shooters with different engines in FPS games, e.g., CS2. However, adaptation is needed for other subgenres, where certain elements like flashes and grenades may not apply. We summarize two core principles for adapting HAWK to other subgenres. (a) *Generalized anti-cheat perspectives transform from three observations.* The fundamental structure of transforming three key observations into three corresponding anti-cheat subsystems is a generalized framework applicable to any FPS subgenre. While the specific features or model architectures within each subsystem may need to be optimized for different games, the principle of using these three complementary perspectives to identify cheating behavior is universally necessary and applicable. (b) *Adaptable feature extraction strategy.* We propose that feature extraction for any FPS game that uses HAWK should be divided into two distinct categories. *Core FPS features.* These are fundamental features inherent to all FPS games and should be retained across all subgenres. For example, this includes data like player position, distance to target, and view direction (in REVPOV); or various aiming speeds, angles, and precision/hit rates (in REVSTATS). While generalizing HAWK to other subgenres, these features are applicable without any modification. *Subgenre-specific features.* These features are designed around the unique mechanics that define a specific subgenre. The design of subgenre-specific features, as well as the classification rules in EXSPC, should be led by senior anti-cheat developers with deep expertise in the specific game.

This ensures the system is tailored to detect cheats that exploit that subgenre’s unique mechanics. For instance, in a Hero Shooter (e.g., *Overwatch*, *Valorant*), the ability to use unique character skills is a key differentiator. To adapt HAWK to other subgenres, one would: i. augment REVPOV with basic temporal information related to skill activation and targeting; ii. extend REVSTATS to record metrics like skill accuracy, the mean and variance of skill usage timing, and their effectiveness.

**Manual involvement.** Although HAWK has significantly increased the detection performance and efficiency, as mentioned in Section III-B, HAWK-after-use manual verification is unavoidable. However, platform statistics indicate their anti-cheat recall (47%) is significantly lower than HAWK’s (79% on average) under recall-first mode. Although HAWK’s false FPR is around 25%, the high recall outweighs the FPR increase (about 15%). A higher FNR indicates more cheaters undetected, leading to user attrition with greater losses than those caused by higher FPR [66]. HAWK also offers Balance mode whose FPR is lower and recall is higher than the current in-use anti-cheat (Section VI-F and Figure 6). Under this mode, HAWK outperforms current anti-cheat and obtains lower manual involvement, due to lower FPR. Note that for any anti-cheat system, all results must undergo manual review and confirmation before any bans are issued (i.e., the GM verification stage). To provide an intuitive demonstration of HAWK’s performance, unless otherwise specified, all results presented for this system are shown before manual review. Therefore, all positive samples mentioned in the evaluation require manual review before any bans can be enforced in actual operation. No player will be mistakenly banned or inconvenienced before the manual revision. Regarding the trade-off between *recall* and *FPR*, we have demonstrated the system’s performance under different anti-cheating requirements in Table VIII. It can be observed that for every approximately 5% increase in *recall*, *FPR* increases by 10% and 20.00% and 20.84% increase of the manpower required on average in terms of the *aimbot* and the *wallhack*, respectively. Therefore, if human resources are relatively scarce, the default or balanced mode of HAWK should be used.

**Dataset imbalance and result significance.** To statistically validate the performance stability of our models, we employed bootstrap resampling [67] with 5,000 iterations to estimate 95% confidence intervals for all evaluation metrics in Table XII. The bootstrap analysis confirmed the statistical significance and robustness of our models under class-imbalanced conditions. All performance metrics showed narrow 95% confidence intervals. This demonstrates that both *aimbot* and *wallhack* detection performances are not only practically meaningful but also statistically reliable, validating the effectiveness of our approach even with inherent dataset imbalances in the context of game anti-cheating.

## VIII. RELATED WORKS

**Server-side anti-cheats.** Yeung et al. [10] initially proposed a Bayesian model to tune the probability threshold with naive features (e.g., whether the player is moving, the distance

TABLE XII: Performance metrics with 95% confidence intervals from bootstrap analysis (5,000 resamples).

Dataset	Metric	Original	Bootstrap_Mean	Std_Dev	Std_Error	CI	CI_Width
Aimbot	Accuracy	0.716149	0.716142	0.00467	0.000066	[0.706972, 0.725323]	0.018351
	Recall	0.726244	0.726073	0.014762	0.000209	[0.697646, 0.755435]	0.057789
	NPV	0.960191	0.960179	0.00249	0.000035	[0.955263, 0.964983]	0.00972
	AUC-ROC	0.72065	0.720535	0.007924	0.000112	[0.704752, 0.736172]	0.03142
	FPR	0.284944	0.284831	0.004967	0.00007	[0.274992, 0.294452]	0.01946
Wallhack	Accuracy	0.756375	0.756422	0.004182	0.000059	[0.748394, 0.764651]	0.016257
	Recall	0.847805	0.847965	0.011178	0.000158	[0.826003, 0.869812]	0.043808
	NPV	0.977897	0.977882	0.001741	0.000025	[0.97437, 0.981204]	0.006834
	AUC-ROC	0.797024	0.797097	0.006064	0.000086	[0.785037, 0.808961]	0.023923
	FPR	0.253757	0.253778	0.004606	0.000065	[0.244804, 0.262858]	0.018054

between the attacker and victim) in 2006, but its performance lacks real-world validation and the features are outdated for today’s advanced cheating techniques and sophistication. Subsequent works [11], [12], [13], [31], [30] employed statistical tests with basic features (e.g., time-on-target) to examine data distribution difference [11], set fixed threshold with limited features (e.g., extra shots count on an invisible bait) [13], [30], or used one machine learning model (e.g., SVM) with basic non-temporal features (e.g., whether the target’s position changed) [12], which couldn’t monitor sophisticated behaviors or describe entire matches [6], or ineffective to certain type of cheat. Due to the scarcity of real-world datasets, these server-side studies relied on private servers and simulated data for evaluation, with the largest dataset containing only 47 cheaters [13]. Such small-scale datasets are insufficient to reflect real-world anti-cheat performance and possibly lead to inconsistent performance between the reported results and real-world performance. Additionally, works like [11], [12], [13], [31] require game engine modifications for concurrent data collection, necessitating significant adaptation efforts after each update and limiting generalizability to other games. Importantly, prior works leverage a single model to classify and could result in biased predictions on the complex real-world dataset as discussed in Section V-B. CUPID [68] is a matchmaking design to optimize the user’s gameplay experience. In terms of anti-cheat, it may be modified to arrange cheaters within the same match so that they would not appear in the normal matches. However, its applicability remains unknown since it does not target identifying cheaters. **Client-side anti-cheats.** BotScreen [6], the latest *aimbot* detector, uses SGX to securely store and run its detection model with temporal aiming features. It constructs its dataset using a self-setup server with 14 players in Deathmatch (gameplay is different from Rank) and evaluates with the deprecated open-source *aimbot* Osiris [69]. This setup may not accurately reflect performance against more sophisticated cheats or common cheating scenarios [70], [71], leaving its real-world functionality unclear. It is also troubled by the deprecated TEE constraint [14], [15]. Invisibility Cloak [8] and BlackMirror [9] only prevent without detecting and are limited to hardware constraints or client overheads, and targeting on a specific cheat subcategory. Commercial anti-cheats like VAC [18], Vanguard [35], EAC [16] and BattlEye [17] offer both detection and prevention [72] for various games through customization. They monitor and manage process privileges, scan DNS caches and cookies for browsing history and cheat purchase records [73], [18], and may use kernel-level drivers [33]. However, these solutions are limited by

security and privacy concerns mentioned in Section I. The common approach of creating blacklists for known cheats and issuing bans based on detected malware signatures [38], [33], [6], [13] is ineffective against new or updated cheats with different signatures [6], [13], lacking robustness to cheat evolutions. Most cheaters avoid using legacy cheats as paid cheats often offer auto-updates to evade bans, leading to low recall in industry anti-cheats, which are always one step behind. These anti-cheats are integrated into games before release and must run concurrently with gameplay [33], causing client overheads and limited generalizability. They also combine multiple methods for cross-checking, extending the banning cycle [33]. Importantly, these commercial anti-cheats are proprietary and closed-source [33], making it infeasible for researchers to conduct comparison studies without collaborating with game vendors. VESPA [74] combines computer vision techniques and human inspection to capture the user’s screen and detect the *wallhack*’s UI overlays and thereby identify cheaters. This may raise privacy concerns and can be easily bypassed by managing process privileges or disabling the visible overlays. Therefore, it is less practical for real-world deployment. FCDGame [75] leverages few-shot learning to learn highly repetitive gesture trajectory patterns on the mobile phone screen to identify cheaters. This pattern targets the bot identification in MMORPGs rather than FPS games. Because the former only requires fixed navigation and simple gesture operations to achieve repetitive tasks (e.g., collect mines), but the latter requires real-time and complex inputs to adjust aiming and perform shooting. The FPS trajectory patterns are more complex and irregular. Therefore, the screen gesture trajectory feature may be less functional in FPS games.

## IX. CONCLUSION

We proposed an FPS games’ server-side anti-cheat framework HAWK, drawing inspiration from how humans identify cheaters. With promising experimental results, we have demonstrated HAWK’s real-world effectiveness, efficiency, and robustness in identifying cheaters in a modern FPS game. Ultimately, we hope HAWK can be a pathfinder for next-generation FPS anti-cheat, providing a valuable dataset and a reference for the follow-up research.

## ACKNOWLEDGMENTS

We thank 5EPlay for sharing and labeling the dataset. We appreciate Associate Editor Prof. Abderrahim Benslimane for arranging the review process, and three anonymous reviewers for their professional reviews. We also acknowledge the anonymous reviewers from IEEE S&P, ACM CCS, USENIX Security and NDSS for their constructive reviews on the past versions of this research paper. This work is partially supported by the NSFC for Young Scientists of China (No.62202400) and the RGC for Early Career Scheme (No.27210024). Any opinions, findings, or conclusions expressed in this material are those of the authors and do not necessarily reflect the views of NSFC and RGC.

## REFERENCES

- [1] Newzoo, "The global games market will generate \$187.7 billion in 2024," <https://newzoo.com/resources/blog/global-games-market-revenue-estimates-and-forecasts-in-2024>, August 2024.
- [2] Irdeto, "Cheating in video games: The A to Z," <https://blog.irdeto.com/video-gaming/cheating-in-games-everything-you-always-wanted-to-know-about-it/>, 2023.
- [3] WePC, "Video Game Industry Statistics, Trends and Data In 2023," <https://www.wepec.com/news/video-game-statistics/>, 2023.
- [4] Z. Belyaeva, A. Petrosyan, and R. Shams, "Stakeholder data analysis in the video gaming industry: Implications for regional development," *EuroMed Journal of Business*, vol. 17, 05 2022.
- [5] S. Liu, M. Claypool, A. Kuwahara, J. Sherman, and J. J. Scovell, "Lower is better? the effects of local latencies on competitive first-person shooter game players," in *Proceedings of the 2021 CHI Conference on Human Factors in Computing Systems*, ser. CHI '21. New York, NY, USA: Association for Computing Machinery, 2021. [Online]. Available: <https://doi.org/10.1145/3411764.3445245>
- [6] M. Choi, G. Ko, and S. K. Cha, "Botscreen: trust everybody, but cut the aimbots yourself," in *Proceedings of the 32nd USENIX Conference on Security Symposium*, ser. SEC '23. USA: USENIX Association, 2023.
- [7] S. Gianvecchio, Z. Wu, M. Xie, and H. Wang, "Battle of botcraft: fighting bots in online games with human observational proofs," in *Proceedings of the 16th ACM Conference on Computer and Communications Security*, ser. CCS '09. New York, NY, USA: Association for Computing Machinery, 2009, p. 256–268. [Online]. Available: <https://doi.org/10.1145/1653662.1653694>
- [8] C. Sun, K. Ye, L. Su, J. Zhang, and C. Qian, "Invisibility cloak: Proactive defense against visual game cheating," in *33rd USENIX Security Symposium (USENIX Security 24)*. Philadelphia, PA: USENIX Association, Aug. 2024, pp. 3045–3061. [Online]. Available: <https://www.usenix.org/conference/usenixsecurity24/presentation/sun-chenxin>
- [9] S. Park, A. Ahmad, and B. Lee, "Blackmirror: Preventing wallhacks in 3d online fps games," in *Proceedings of the 2020 ACM SIGSAC Conference on Computer and Communications Security*, ser. CCS '20. New York, NY, USA: Association for Computing Machinery, 2020, p. 987–1000. [Online]. Available: <https://doi.org/10.1145/3372297.3417890>
- [10] S. Yeung, J. Lui, J. Liu, and J. Yan, "Detecting cheaters for multiplayer games: theory, design and implementation," in *CCNC 2006. 2006 3rd IEEE Consumer Communications and Networking Conference, 2006.*, vol. 2. Las Vegas, NV, USA: IEEE, 2006, pp. 1178–1182.
- [11] S.-Y. Yu, N. Hammerla, J. Yan, and P. Andras, "A statistical aimbot detection method for online fps games," in *The 2012 International Joint Conference on Neural Networks (IJCNN)*. Brisbane, QLD, Australia: IEEE, 2012, pp. 1–8.
- [12] H. Alayed, F. Frangoudes, and C. Neuman, "Behavioral-based cheating detection in online first person shooters using machine learning techniques," in *2013 IEEE Conference on Computational Intelligence in Games (CIG)*. Niagara Falls, ON, Canada: IEEE, Aug 2013, pp. 1–8.
- [13] D. Liu, X. Gao, M. Zhang, H. Wang, and A. Stavrou, "Detecting passive cheats in online games via performance-skillfulness inconsistency," in *2017 47th Annual IEEE/IFIP International Conference on Dependable Systems and Networks (DSN)*. Denver, CO, USA: IEEE, 2017, pp. 615–626.
- [14] BleepingComputer, "New intel chips won't play blu-ray disks due to sgx deprecation," <https://www.bleepingcomputer.com/news/security/new-intel-chips-wont-play-blu-ray-disks-due-to-sgx-deprecation/>, Bleeping Computer LLC, 2022, Accessed: 2024-02-27.
- [15] Intel Community, "Rising to the challenge: Data security with intel confidential," <https://community.intel.com/t5/Blogs/Products-and-Solutions/Security/Rising-to-the-Challenge-Data-Security-with-Intel-Confidential/post/1353141>, 2022, Accessed: 2024-02-27.
- [16] Epic Games, Inc., "Easy Anti-Cheat," <https://www.easy.ac/>, 2024.
- [17] BattlEye Innovations, "Interested in using BattlEye?" <https://www.battleye.com/>, 2024.
- [18] V. Corporation, "Valve anti-cheat (vac) system," <https://help.steampowered.com/en/faqs/view/571A-97DA-70E9-FF74>, 2023.
- [19] K. K. Mikkelsen, "Information security as a countermeasure against cheating in video games," Master's thesis, NTNU, 2017.
- [20] A. Maario, V. K. Shukla, A. Ambikapathy, and P. Sharma, "Redefining the risks of kernel-level anti-cheat in online gaming," in *2021 8th International Conference on Signal Processing and Integrated Networks (SPIN)*. Noida, India: IEEE, 2021, pp. 676–680.
- [21] T. Witschel and C. Wressnegger, "Aim low, shoot high: Evading aimbot detectors by mimicking user behavior," in *Proceedings of the 13th European Workshop on Systems Security*, ser. EuroSec '20. New York, NY, USA: Association for Computing Machinery, 2020, p. 19–24. [Online]. Available: <https://doi.org/10.1145/3380786.3391397>
- [22] bright, IDontCode, irql0, "EasyAntiCheat Exploit to inject unsigned code into protected processes," <https://blog.back.engineering/10/08/2021/>, August 2021, Accessed: 2024-02-29.
- [23] CVE-2019-16098, "CVE-2019-16098: Vulnerability in MSI Afterburner," <https://nvd.nist.gov/vuln/detail/CVE-2019-16098>, 2019, Accessed: 2023-12-07.
- [24] CVE-2020-36603, "CVE-2020-36603: Vulnerability in Genshin Impact Anti-Cheat Software," <https://nvd.nist.gov/vuln/detail/CVE-2020-36603>, 2022, Accessed: 2023-12-07.
- [25] CVE-2021-3437, "CVE-2021-3437: HP OMEN Gaming Hub Privilege Escalation Bug Hits Millions of Gaming Devices," <https://www.sentinelone.com/labs/cve-2021-3437-hp-omen-gaming-hub-privilege-escalation-bug-hits-millions-of-gaming-devices/>, 2021, Accessed: 2023-12-07.
- [26] CVE-2023-38817, "CVE-2023-38817: Vulnerability in Minecraft Anti-Cheat Tool," <https://nvd.nist.gov/vuln/detail/CVE-2023-38817>, 2023, Accessed: 2023-12-07.
- [27] G. on Games, "Never trust the client," 2016, accessed: 2024-12-20. [Online]. Available: <https://web.archive.org/web/20170510170653/https://gafferrongames.com/2016/04/25/never-trust-the-client/>
- [28] K. Stuart, "How hackers and cheats ruined the division on pc," *The Guardian*, 2016, accessed: 2024-12-20. [Online]. Available: <https://www.theguardian.com/technology/2016/apr/26/hackers-cheats-ruined-the-division-pc-ubisoft>
- [29] i3D.net, "Countering the scourge of cheating in games," 2024, accessed: 2024-12-20. [Online]. Available: <https://www.i3d.net/countering-scurge-of-cheating-in-games/>
- [30] J. Orlova, A. Stepanov, A. Vinogradov, L. Orlova, A. Baldycheva, and A. Somov, "Estimation of in-game player behavior by measuring key gameplay parameters," in *2024 IEEE International Instrumentation and Measurement Technology Conference (I2MTC)*. IEEE, 2024, pp. 1–6.
- [31] M. L. Han, J. K. Park, and H. K. Kim, "Online game bot detection in fps game," in *Proceedings of the 18th Asia Pacific Symposium on Intelligent and Evolutionary Systems-Volume 2*. Springer, 2015, pp. 479–491.
- [32] JARVIS THE NPC, "Warzone Reddit Outcry: Anti-Cheat Failures Fuel Frustration Among Players," <https://www.zleague.gg/theportal/warzone-reddit-outcry-anti-cheat-failures-fuel-frustration-among-players/>, April 2024, Accessed: 2024-04-24.
- [33] R. K. RIGNEY, "The gamers do not understand anti-cheat," <https://www.pushtotalk.gg/p/the-gamers-do-not-understand-anti-cheat>, February 2024, Accessed: 2024-04-24.
- [34] B. Toulas, "Apex Legends players worried about RCE flaw after ALGS hacks," <https://www.bleepingcomputer.com/news/security/apex-legends-players-worried-about-rce-flaw-after-algs-hacks/>, March 2024, Accessed: 2024-04-08.
- [35] R. G. Inc., "What is vanguard?" <https://support.valorant.riotgames.com/hc/en-us/articles/360046160933-What-is-Vanguard->, Jun 2022.
- [36] L. WELLBIA.COM CO., "Wellbia," <https://wellbia.com/>, 2023.
- [37] S. Fei, Z. Yan, W. Ding, and H. Xie, "Security vulnerabilities of sgx and countermeasures: A survey," *ACM Comput. Surv.*, vol. 54, no. 6, jul 2021. [Online]. Available: <https://doi.org/10.1145/3456631>
- [38] A. Kanervisto, T. Kinnunen, and V. Hautamäki, "Gan-aimbots: Using machine learning for cheating in first person shooters," *IEEE Transactions on Games*, vol. 15, no. 4, pp. 566–579, 2023.
- [39] L. Galli, D. Loiacono, L. Cardamone, and P. L. Lanzi, "A cheating detection framework for unreal tournament iii: A machine learning approach," in *2011 IEEE Conference on Computational Intelligence and Games (CIG'11)*. Seoul, Korea (South): IEEE, 2011, pp. 266–272.
- [40] AFK Gaming, "8 types of hacks and cheats in CS:GO," <https://afkgaming.com/csgo/news/2619-8-types-of-hacks-and-cheats-in-csgo>, 2019.
- [41] M. Consalvo, *Cheating: Gaining Advantage in Videogames*. Cambridge, MA: MIT Press, 2007.
- [42] S. Hochreiter and J. Schmidhuber, "Long short-term memory," *Neural Computation*, vol. 9, no. 8, pp. 1735–1780, 1997.
- [43] N. Srivastava, G. Hinton, A. Krizhevsky, I. Sutskever, and R. Salakhutdinov, "Dropout: A simple way to prevent neural networks from overfitting," *J. Mach. Learn. Res.*, vol. 15, no. 1, p. 1929–1958, jan 2014.
- [44] M.-T. Luong, H. Pham, and C. D. Manning, "Effective approaches to attention-based neural machine translation," 2015.
- [45] S. Haykin, *Neural networks: a comprehensive foundation*. USA: Prentice Hall PTR, 1994.
- [46] J. S. Cramer, "The origins of logistic regression," Tinbergen Institute, Tinbergen Institute Discussion Papers 02-119/4, 2002.

- [47] L. Breiman, "Random forests," *Machine learning*, vol. 45, pp. 5–32, 2001.
- [48] C. Cortes and V. Vapnik, "Support-vector networks," *Machine learning*, vol. 20, pp. 273–297, 1995.
- [49] K. P. Murphy *et al.*, "Naive bayes classifiers," *University of British Columbia*, vol. 18, no. 60, pp. 1–8, 2006.
- [50] G. H. John and P. Langley, "Estimating continuous distributions in bayesian classifiers," in *Proceedings of the Eleventh Conference on Uncertainty in Artificial Intelligence*, ser. UAI'95. San Francisco, CA, USA: Morgan Kaufmann Publishers Inc., 1995, p. 338–345.
- [51] S. Srivastava, M. R. Gupta, and B. A. Frigiyik, "Bayesian quadratic discriminant analysis," *Journal of Machine Learning Research*, vol. 8, no. 46, pp. 1277–1305, 2007. [Online]. Available: <http://jmlr.org/papers/v8/srivastava07a.html>
- [52] P. Xenopoulos, "awpy: A Python package for Counter-Strike: Global Offensive data parsing, analytics, and visualization," <https://awpy.readthedocs.io/en/latest/>, 2023, Accessed: 2025-02-21.
- [53] T. Elomaa and M. Kaariainen, "An analysis of reduced error pruning," *Journal of Artificial Intelligence Research*, vol. 15, pp. 163–187, 2001.
- [54] G. Góra and A. Wojna, "Riona: A classifier combining rule induction and k-nn method with automated selection of optimal neighbourhood," in *Machine Learning: ECML 2002: 13th European Conference on Machine Learning Helsinki, Finland, August 19–23, 2002 Proceedings 13*. Berlin, Heidelberg: Springer, 2002, pp. 111–123.
- [55] D. Yates, M. Z. Islam, and J. Gao, "Spaarc: a fast decision tree algorithm," in *Data Mining: 16th Australasian Conference, AusDM 2018, Bahrurst, NSW, Australia, November 28–30, 2018, Revised Selected Papers 16*. Singapore: Springer, 2019, pp. 43–55.
- [56] L. Breiman, "Bagging predictors," *Machine Learning*, vol. 24, no. 2, pp. 123–140, 1996.
- [57] G. Demiröz and H. A. Güvenir, "Classification by voting feature intervals," in *European Conference on Machine Learning*. Berlin, Heidelberg: Springer, 1997, pp. 85–92.
- [58] W. W. Cohen, "Fast effective rule induction," in *Proceedings of the Twelfth International Conference on International Conference on Machine Learning*, ser. ICML'95. San Francisco, CA, USA: Morgan Kaufmann Publishers Inc., 1995, p. 115–123.
- [59] J. Stefanowski, *On Combined Classifiers, Rule Induction and Rough Sets*. Berlin, Heidelberg: Springer, 2007, pp. 329–350. [Online]. Available: [https://doi.org/10.1007/978-3-540-71200-8\\_18](https://doi.org/10.1007/978-3-540-71200-8_18)
- [60] M. J. Siers and M. Z. Islam, "Software defect prediction using a cost sensitive decision forest and voting, and a potential solution to the class imbalance problem," *Information Systems*, vol. 51, pp. 62–71, 2015.
- [61] DatHost, "CS2 Server Hosting," <https://dathost.net/cs2-server-hosting>, 2024, Accessed: 2024-06-05.
- [62] SteamDB, "Counter-Strike 2 Steam Charts," <https://steamdb.info/app/730/charts/#48h>, 2024, Accessed: 2024-06-05.
- [63] J. Zheng, C. Xiao, M. Li, Z. Li, F. Qian, W. Liu, and X. Wu, "Parlirobo: Participant lightweight ai robots for massively multiplayer online games (mmogs)," in *Proceedings of the 31st ACM International Conference on Multimedia*, ser. MM '23. New York, NY, USA: Association for Computing Machinery, 2023, p. 9093–9102. [Online]. Available: <https://doi.org/10.1145/3581783.3613764>
- [64] M. Kerrisk, "time(1) — Linux manual page," <https://man7.org/linux/man-pages/man1/time.1.html>, 2024, Accessed: 2024-06-05.
- [65] Wikipedia, "Tactical shooter," [https://en.wikipedia.org/wiki/Tactical\\_shooter](https://en.wikipedia.org/wiki/Tactical_shooter), 2024, Accessed: 2024-06-14.
- [66] J. Tao, Y. Xiong, S. Zhao, R. Wu, X. Shen, T. Lyu, C. Fan, Z. Hu, S. Zhao, and G. Pan, "Explainable ai for cheating detection and churn prediction in online games," *IEEE Transactions on Games*, vol. 15, no. 2, pp. 242–251, 2023.
- [67] B. Efron, "Bootstrap methods: Another look at the jackknife," *The Annals of Statistics*, vol. 7, no. 1, pp. 1–26, 1979. [Online]. Available: <http://www.jstor.org/stable/2958830>
- [68] G. Fan, C. Zhang, K. Wang, Y. Li, J. Chen, and Z. Xu, "Cupid: Improving battle fairness and position satisfaction in online moba games with a re-matchmaking system," *Proc. ACM Hum.-Comput. Interact.*, vol. 8, no. CSCW2, Nov. 2024. [Online]. Available: <https://doi.org/10.1145/3686978>
- [69] D. Krupiński, "Osiris," <https://github.com/danielkrupinski/Osiris>, 2023, Accessed: 2024-02-27.
- [70] Mike Scorpio, "What You Should Know About Aimbots Before Using Them in a Video Game," <https://miketendo64.com/2021/01/07/what-you-should-know-about-aimbots-before-using-them-in-a-video-game/>, January 2021, Accessed: 2024-06-13.
- [71] m2qchqo110, "The Most Hilarious Complaints We've Heard About PUBG Aimbots," <https://medium.com/@p5hvlpr124/the-most-hilarious-complaints-weve-heard-about-pubg-aimbot-b596bbcb1ce5>, August 2019, Accessed: 2024-06-13.
- [72] J. N. Silva, "Towards automated server-side video game cheat detection," <https://repositorio-aberto.up.pt/bitstream/10216/142935/2/572983.pdf>, July 2022.
- [73] S. Lehtonen *et al.*, "Comparative study of anti-cheat methods in video games," *University of Helsinki, Faculty of Science*, 2020.
- [74] S. Zhao, J. Qi, Z. Hu, H. Yan, R. Wu, X. Shen, T. Lv, and C. Fan, "Vespa: A general system for vision-based extrasensory perception anticheeling in online fps games," *IEEE Transactions on Games*, vol. 16, no. 3, pp. 611–620, 2024.
- [75] Y. Su, D. Yao, X. Chu, W. Li, J. Bi, S. Zhao, R. Wu, S. Zhang, J. Tao, and H. Deng, "Few-shot learning for trajectory-based mobile game cheating detection," in *Proceedings of the 28th ACM SIGKDD Conference on Knowledge Discovery and Data Mining*, ser. KDD '22. New York, NY, USA: Association for Computing Machinery, 2022, p. 3941–3949. [Online]. Available: <https://doi-org.eproxy.lib.hku.hk/10.1145/3534678.3539157>

# Identify As A Human Does: A Pathfinder of Next-Generation Anti-Cheat Framework for First-Person Shooter Games

Jiayi Zhang<sup>1</sup>, Chenxin Sun<sup>1</sup>, Yue Gu<sup>1</sup>, Qingyu Zhang<sup>1</sup>, Jiayi Lin<sup>1</sup>, Xiaojiang Du<sup>1</sup>, Chenxiong Qian<sup>1</sup>

## A. Ethics Considerations

The dataset only contains publicly accessible information including in-game operations and data, and the banning information. Its publication ensures no direct or indirect harm to the game, its distributors, players, or the community. The data provider has approved its release and reuse for research purposes, and no private information will be disclosed. Still, we anonymized all information to minimize the probability of causing any unforeseen privacy concerns. A data usage agreement will require users to commit to ethical, academic, and non-malicious use, with clear guidelines provided on ethical use and potential risks before using. The study adheres to local legislation and institutional requirements.

TABLE I: Experts' skill level for sampled match review, all stats are retrieved from [1].

Expert	Playtime	Skill Level
#1	>7,000hrs	CS:GO - Premier 19,000 (Top 2.62%) Overwatch2 - Role Grand Master (Top 1.46%) Apex Legend - BR Master (Top 0.6%)
#2	>1,400hrs	CS:GO - Premier 19,200 (Top 2.62%)
#3	>5,000hrs	CS:GO - Premier 18,000 (Top 4.59%)

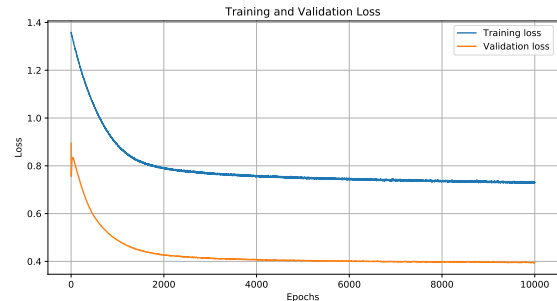
## B. Training and Validation Loss for EXSPC Model

The training process on each of the datasets in EXSPC utilizes the validation set for optimization. Figure 1a and Figure 1b demonstrate the training and validation loss for each dataset, respectively. It is noticeable that the performance result of EXSPC is not as ideal as HAWK, although it utilizes both REVPOV and REVSTATS's inputs. And thereby prove the need for all three subsystems as well as the TSTO. Thus, we use the multi-view design to complement one another of the subsystems.

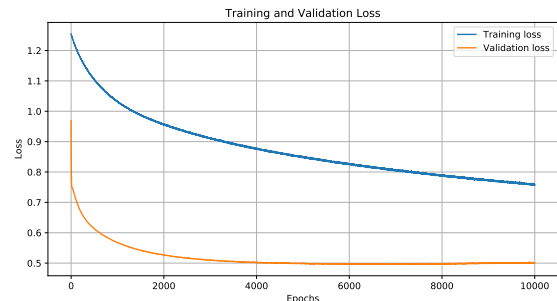
## C. Structured Features

In this section, the extracted data from demos are further processed to create strong-expressiveness features that can indicate the sense and performance of a player clearly. For notations used in the formulas throughout this section, please refer to Table II. [S] denotes that the feature is a subgenre-specific feature, and [C] denotes that the feature is an FPS core feature mentioned in Section VII.

### 1) Aiming features:



(a) Wallhack dataset



(b) Aimbot dataset

Fig. 1: Training and validation loss of EXSPC on two datasets: Wallhack (a) and Aimbot (b).

**Durations:** Figure 2 illustrates the three distinct moments that form three different durations. In terms of the moments,  $t_0$  denotes the moment that the current player initially spots one opponent. In Figure 2, a1 and a2 present a possible set of states at  $t_0$ . In which a1 represents a 3-dimensional world in the game map, where the opponent happens to appear at the edge of the current player's field of view (FOV). And a2 demonstrates the 2-dimensional state correspondingly which is typically displayed through the player's monitor, where the opponent also happens to be spotted at the edge of the current player's POV.  $t_1$  denotes the moment that the current player notices the hostile movement and initiates responsive action (*i.e.*, open fire). Note that at  $t_1$  the current firing event may or may not be equivalent to a damage event upon the opponent.  $t_2$  denotes the moment that the current player performs a damage event upon the opponent within one period of valid engagement for the first time. In our case, the threshold for resetting the valid engagement period detection (*i.e.*, no opponent in sight, no damage or firing event) is set as 10 seconds. In Figure 2, it demonstrates a series of generic circumstances that often happen in games where the positions of the current player and

TABLE II: Notations and descriptions of structured features.

Notation	Description	Notation	Description
$i$	the current player	$\mathbf{E}_x^{a \rightarrow b}[k]$	the $k^{\text{th}}$ type $x$ event conducted by player $a$ to $b$
$p, p^*$	a particular player, any player	$\#(\bullet)$	the number of counts of the parameter
$o, o^*$	a particular opponent, any opponent	$wp(\bullet)$	the weapon used by a player
$a, a^*$	a particular ally, any ally	$hg(\bullet)$	the body part hit by a player
$ts$	through smoke	$t(\bullet)$	the moment of the event occurs in second
$p(\bullet)$	the number of occluders penetrated	$mag(\bullet)$	the number of bullets remain in a player's magazine
$\Delta(\bullet)$	the change in the parameter	$dist(x, y)$	the distance range between entities $x$ and $y$
<b>ELAPSE</b> ( $\bullet$ )	the duration from the start to the end of an event	<b>HEG</b> ( $\bullet$ )	high-explosive grenade is applied by a player
<b>INC</b> ( $\bullet$ )	incendiary or Molotov is applied by a player	<b>SMK</b> ( $\bullet$ )	smoke grenade is applied by a player
<b>FLS</b> ( $\bullet$ )	flash grenade is applied by a player	<b>FK</b> ( $\bullet$ )	first kill is accomplished by a player

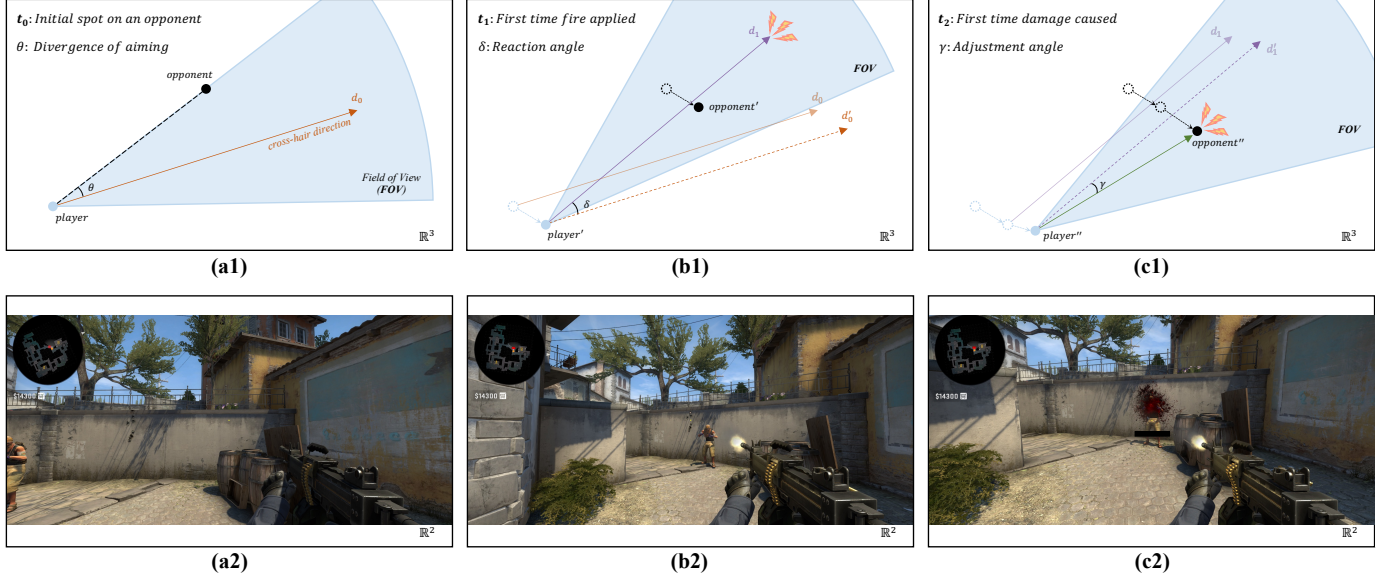


Fig. 2: Illustrations of reaction and adjustment features. The black rectangle overlay in c2 hides the player's ID.

the opponent vary along from  $t_0$  to  $t_2$ . And it is common that sometimes  $t_1$  and  $t_2$  are overlapped. In terms of durations, the elapsed period from  $t_0$  to  $t_1$  is defined as *reaction time* (*rat*). The elapsed period from  $t_1$  to  $t_2$  is defined as *adjustment time* (*ajt*). The elapsed period from  $t_0$  to  $t_2$  is defined as *duration time* (*drt*). The average and variance calculations are applied after obtaining the data. The average performance of all samples is obtained through the average, and the degree of dispersion of the samples is represented by the variance. The integration of average and variance is able to represent the overall performance and stability of the current player within a match.

*rat average*. [C] Denotes the average performance regarding *rat* of the current player among one match. The lower this feature is, the faster the player reacts.

$$\mathbf{F}_{\text{rat-avg}}(\mathbf{i}) = \overline{RAT} = \frac{\sum_{j=1}^N RAT_j}{N} \quad (1)$$

where  $N$  denotes  $\#(RAT)$  within a match.

*rat variance*. [C] Denotes the degree of dispersion of *rat* distributions of the current player among one match.

$$\mathbf{F}_{\text{rat-var}}(\mathbf{i}) = \text{Var}(RAT) = \frac{\sum_{j=1}^N (RAT_j - \overline{RAT})^2}{N} \quad (2)$$

where  $N$  denotes  $\#(RAT)$  within a match.

*ajt average*. [C] Denotes the average performance regarding *ajt* of the current player among one match. The lower this feature is, the faster the player adjusts.

$$\mathbf{F}_{\text{ajt-avg}}(\mathbf{i}) = \overline{AJT} = \frac{\sum_{j=1}^N AJT_j}{N} \quad (3)$$

where  $N$  denotes  $\#(AJT)$  within a match.

*ajt variance*. [C] Denotes the degree of dispersion of *ajt* distributions of the current player among one match.

$$\mathbf{F}_{\text{ajt-var}}(\mathbf{i}) = \text{Var}(AJT) = \frac{\sum_{j=1}^N (AJT_j - \overline{AJT})^2}{N} \quad (4)$$

where  $N$  denotes  $\#(AJT)$  within a match.

*drt average*. [C] Denotes the average performance regarding *drt* of the current player among one match. The lower this feature is, the faster the player hits.

$$\mathbf{F}_{\text{drt-avg}}(\mathbf{i}) = \overline{DRT} = \frac{\sum_{j=1}^N DRT_j}{N} \quad (5)$$

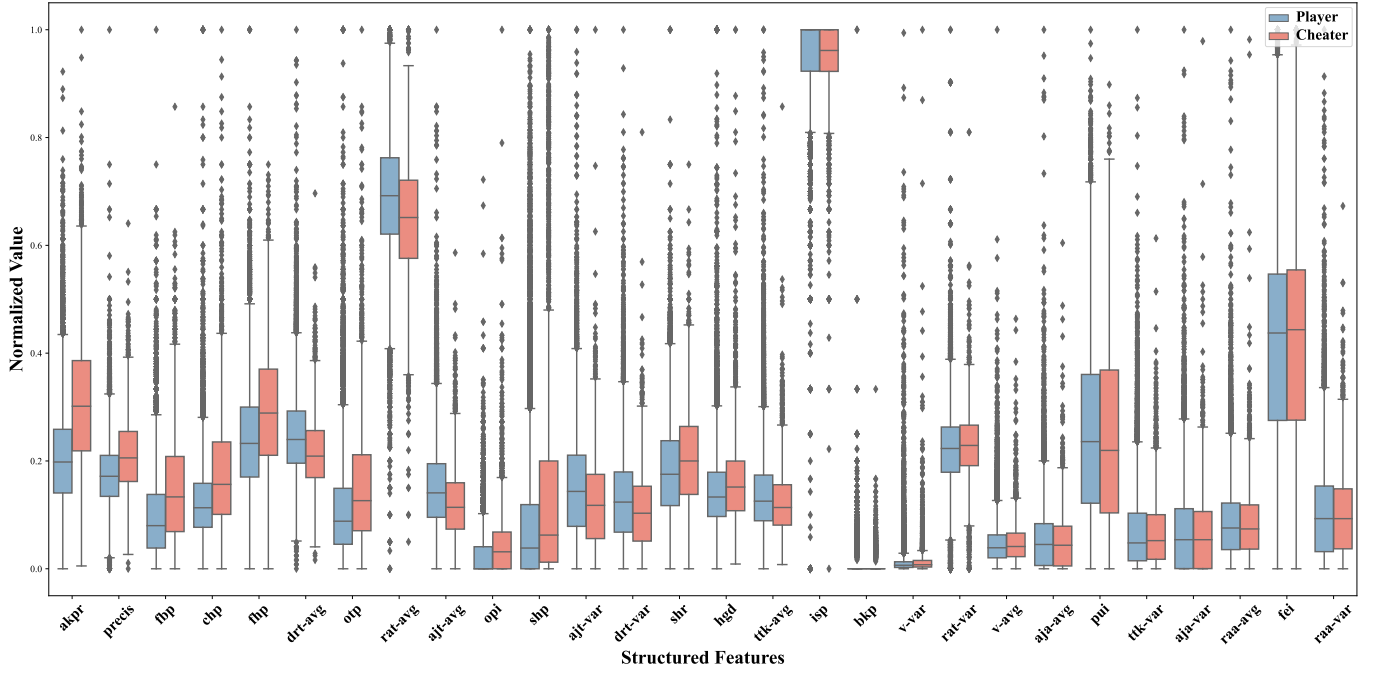


Fig. 3: Complete box plots of comparative visualization between honest players and cheaters on all structured features under Mann-Whitney U (Wilcoxon Rank-Sum) test with P-Value ascending (distinction descending) order.

*drt variance.* [C] Denotes the degree of dispersion of *drt* distributions of the current player among one match.

$$\mathbf{F}_{\text{drt-var}}(\mathbf{i}) = \text{Var}(DRT) = \frac{\sum_{j=1}^N (DRT_j - \overline{DRT})^2}{N} \quad (6)$$

where  $N$  denotes  $\#(DRT)$  occurrences within a match.

*Velocity: velocity average.* [C] Denotes the average mouse velocity of the current player among one match between  $t_0$  and  $t_2$ , through which way two features of distance and time period can be highly compressed into one feature. The higher the feature is, the faster the player hits the targets.

$$V = \frac{\text{dist}(i, o)}{DRT_i} \quad (7)$$

where  $o$  denotes the victim in the specified *DRT*.

$$\mathbf{F}_{\text{v-avg}}(\mathbf{i}) = \bar{V} = \frac{\sum_{j=1}^N V_j}{N} \quad (8)$$

where  $N$  denotes  $\#(DRT)$  within a match.

*velocity variance.* [C] Denotes the degree of dispersion of *velocity* distributions of the current player among one match.

$$\mathbf{F}_{\text{v-var}}(\mathbf{i}) = \text{Var}(V) = \frac{\sum_{j=1}^N (V_j - \bar{V})^2}{N} \quad (9)$$

where  $N$  denotes  $\#(DRT)$  within a match.

*Angles:* Figure 2 illustrates the three different angles, in which  $\theta$  denotes *divergence of aiming* is extracted by Liu et al. [2] and represents the initial angular divergence between the aiming position and the opponent position. However, the time complexity for obtaining such a feature is too expensive to be accepted for industrial implementation. Therefore we extracted the following features which not only preserve strong expressiveness but also significantly reduce the time cost, as well as innovatively segment each engagement process into three stages.  $\delta$  represents the *reaction angle (raa)*, which reflects the angle of two cross-hair directions at  $t_0$  and  $t_1$  respectively.  $\gamma$  represents the *adjustment angle (aja)*, which, similarly reflects the angle of two cross-hair directions at  $t_1$  and  $t_2$  respectively. The larger  $\delta$  and  $\gamma$  are the longer distance the cross-hair travels, which ultimately results in performance divergence. Similarly, the average and variance operation is applied accordingly.

*raa average.* [C] Denotes the average performance regarding *raa* of the current player among one match. The lower the feature is, the smaller the angle and the less effort the player aims for and puts into reaching their targets.

$$\mathbf{F}_{\text{raa-avg}}(\mathbf{i}) = \overline{RAA} = \frac{\sum_{j=1}^N RAA_j}{N} \quad (10)$$

where  $N$  denotes  $\#(RAA)$  within a match.

*raa variance.* [C] Denotes the degree of dispersion of *raa* distributions of the current player among one match.

$$\mathbf{F}_{\text{raa-var}}(\mathbf{i}) = \text{Var}(RAA) = \frac{\sum_{j=1}^N (RAA_j - \overline{RAA})^2}{N} \quad (11)$$

where  $N$  denotes  $\#(RAA)$  within a match.

*aja average*. [C] Denotes the average performance regarding *aja* of the current player among one match. The lower the feature is, the smaller angle and the less effort the player fires for and puts into hitting their targets.

$$\mathbf{F}_{\text{aja-avg}}(\mathbf{i}) = \overline{AJA} = \frac{\sum_{j=1}^N AJA_j}{N} \quad (12)$$

where  $N$  denotes  $\#(AJA)$  within a match.

*aja variance*. [C] Denotes the degree of dispersion of *aja* distributions of the current player among one match.

$$\mathbf{F}_{\text{aja-var}}(\mathbf{i}) = \text{Var}(AJA) = \frac{\sum_{j=1}^N (AJA_j - \overline{AJA})^2}{N} \quad (13)$$

where  $N$  denotes  $\#(AJA)$  within a match.

## 2) Firing features:

*Inertial shot [2] percentage (isp)*: *Inertial shot* [C] denotes that after an elimination is conducted by a player, who may apply several extra firings due to the inertia. *isp* represents the ratio of the number of *Inertial shot* times to the number of eliminations.  $\alpha$  is a threshold and set as 0.15 seconds in our case.

$$\mathbf{IS}(\mathbf{E}_{\text{kill}}^{i \rightarrow o^*}[k]) = \begin{cases} 1, & \exists \mathbf{E}_{\text{fire}}^i \in (\mathbf{t}(\mathbf{E}_{\text{kill}}^{i \rightarrow o^*}[k]), \mathbf{t}(\mathbf{E}_{\text{kill}}^{i \rightarrow o^*}[k]) + \alpha) \\ 0, & \text{otherwise} \end{cases} \quad (14)$$

$$\mathbf{F}_{\text{isp}}(\mathbf{i}) = \frac{\sum_k \mathbf{IS}(\mathbf{E}_{\text{kill}}^{i \rightarrow o^*}[k])}{\sum_n \mathbf{E}_{\text{kill}}^{i \rightarrow o^*}[n]} \quad (15)$$

*First hit percentage (fhp)*: [C] Denote how accurate a player is while spotting an opponent and reacting to fire. Event *reload* represents the action of changing the magazine while the firing is performed and the bullet is consumed. *Fire Round* denotes the unit of the firing round. *fhp* refers to the ratio of the number of the first firing event equivalent to a damage event while spotting at least one opponent within a time threshold  $\varepsilon$  to the number of times that the aforementioned event occurs while disregarding the equivalency and within the same time threshold  $\varepsilon$ . In our case,  $\varepsilon$  is set as 5 seconds (*i.e.*, 640 ticks).

$$\mathbf{E}_{\text{reload}}^i = \Delta(\text{mag}(i)) > 0 \wedge \mathbf{t}(\mathbf{E}_{\text{fire}}^i[k]) - \mathbf{t}(\mathbf{E}_{\text{fire}}^i[k+1]) > 0 \quad (16)$$

$$\mathbf{FR}[i] = \{\mathbf{E}_{\text{fire}}^i[i] \mid \exists \mathbf{E}_{\text{reload}}^i \vee \mathbf{t}(\mathbf{E}_{\text{fire}}^i[i][k+1]) - \mathbf{t}(\mathbf{E}_{\text{fire}}^i[i][k]) > \varepsilon\} \quad (17)$$

$$\mathbf{F}_{\text{fhp}}(\mathbf{i}) = \frac{\#\left(\{\mathbf{FR}[i][0] \mid \forall \mathbf{FR}[i][0] = \mathbf{E}_{\text{damage}}^{i \rightarrow o^*}\}\right)}{\#\left(\mathbf{FR}[i][0]\right)} \quad (18)$$

*Precision (precis)*: [C] Denote the performance of firing accuracy. *precis* refers to the ratio of the number of damage caused by weapons to the total number of fires applied.

$$\mathbf{F}_{\text{precis}}(\mathbf{i}) = \frac{\sum_k \mathbf{E}_{\text{damage}}^{i \rightarrow o^*}[k]}{\sum_n \mathbf{E}_{\text{fire}}^i[n]} \quad (19)$$

*Strafing hit percentage (shp)*: [C] Denote fire accuracy while *strafing*. *Strafe* allows a player to keep the view focused on an opponent while moving in a different direction. *shp* refers to the ratio of the number of damage caused while strafing to the number of damage caused.

$$\mathbf{F}_{\text{shp}}(\mathbf{i}) = \frac{\sum_k \mathbf{E}_{\text{damage} \wedge \text{strafe}}^{i \rightarrow o^*}[k]}{\sum_n \mathbf{E}_{\text{damage}}^{i \rightarrow o^*}[n]} \quad (20)$$

*Hit-group distribution (hgd) variance*: [C] *Hit group* represents the body part that suffers damage, typically hit groups can be categorized as follows: *chest*, *generic*, *head*, *neck*, *left arm*, *right arm*, *left leg*, *right leg*, and *stomach*. *hgd* variance denotes the degree of dispersion of *hit group* distributions for the current player among one match.

$$HG_j = \sum_k \mathbf{E}_{\text{damage} \wedge \text{hg}(j)}^{i \rightarrow o^*}[k] \quad (21)$$

$$\overline{HG} = \frac{\sum_{j=\text{chest}}^{\text{stomach}} HG_j}{\sum_k \mathbf{E}_{\text{damage}}^{i \rightarrow o^*}[k]} \quad (22)$$

$$\mathbf{F}_{\text{hgd}}(\mathbf{i}) = \text{Var}(HG) = \frac{\sum_{j=\text{chest}}^{\text{stomach}} (HG_j - \overline{HG})^2}{\sum_n \mathbf{E}_{\text{damage}}^{i \rightarrow o^*}[n]} \quad (23)$$

where  $j \in \{\text{chest, generic, head, neck, left arm, right arm, left leg, right leg, stomach}\}$

*Special hit Ratio (shr)*: [S] *Special hit* denotes hit with sniper between 50 and 150 meters (*SH50-150*), head shot with sniper between 40 and 170 meters (*SHS40-170*), hit with normal weapon farther than 800 meters (*NH800+*) and headshot with normal weapon farther than 700 meters (*NHS700+*). In FPS games, hitting processes include using different weapons and shooting from different distances. In our game environment, the aforementioned four types of hits are considered to be potentially cheating combinations. *shr* denotes the ratio of the sum of the number of the aforementioned four types of *special hit* to the number of hits in one match.

$$\mathbf{SH}_{50-150}(\mathbf{i}) = \sum_k \mathbf{E}_{\text{damage} \wedge \text{sniper} \wedge (50 \leq \text{dist}(i,o) \leq 150)}^{i \rightarrow o^*}[k] \quad (24)$$

$$\mathbf{SHS}_{40-170}(\mathbf{i}) = \sum_k \mathbf{E}_{\text{headshot} \wedge \text{sniper} \wedge (40 \leq \text{dist}(i,o) \leq 170)}^{i \rightarrow o^*}[k] \quad (25)$$

$$\mathbf{NH}_{800+}(\mathbf{i}) = \sum_k \mathbf{E}_{\text{damage} \wedge \text{normal} \wedge (\text{dist}(i,o) > 800)}^{i \rightarrow o^*}[k] \quad (26)$$

$$\mathbf{NHS}_{700+}(\mathbf{i}) = \sum_k \mathbf{E}_{\text{headshot} \wedge \text{normal} \wedge (\text{dist}(i,o) > 700)}^{i \rightarrow o^*}[k] \quad (27)$$

$$\mathbf{F}_{\text{shr}}(\mathbf{i}) = \frac{\mathbf{SH}_{50-150}(\mathbf{i}) + \mathbf{SHS}_{40-170}(\mathbf{i}) + \mathbf{NH}_{800+}(\mathbf{i}) + \mathbf{NHS}_{700+}(\mathbf{i})}{\sum_k \mathbf{E}_{\text{damage}}^{i \rightarrow o^*}[k]} \quad (28)$$

## 3) Elimination features:

*Time to kill (ttk)*: Denote the duration from the moment of the first damage caused to an opponent to the moment of the elimination of the opponent. In order to control the *ttk* to be each time one player attacks one enemy, the threshold of one statistical period of *ttk* is set to be 10 seconds. For instance, if the attacking period time is over 10 seconds without killing the victims, this action time will not be recorded as *ttk*.

$$\mathbf{F}_{\text{ttk}}(\mathbf{i}) = \mathbf{ELAPSE}(\mathbf{E}_{\text{damage}}^{i \rightarrow o}[0], \mathbf{E}_{\text{kill}}^{i \rightarrow o}) \quad (29)$$

*ttk average*. [C] Denotes the average time regarding *ttk* of the current player among one match. The lower this feature is, the shorter the time the player kills victims.

$$\mathbf{F}_{\text{ttk-avg}}(\mathbf{i}) = \overline{TTK} = \frac{\sum_{j=1}^N TTK_j}{N} \quad (30)$$

where  $N$  denotes  $\#(TTK)$  within a match.

*ttk variance*. [C] Denotes the degree of dispersion of *ttk* distributions of the current player among one match.

$$\mathbf{F}_{\text{ttk-var}}(\mathbf{i}) = \text{Var}(TTK) = \frac{\sum_{j=1}^N (TTK_j - \overline{TTK})^2}{N} \quad (31)$$

where  $N$  denotes  $\#(TTK)$  within a match.

*First-blood percentage (fbp)*: [C] *first-blood* denotes the very first elimination in one round. *fbp* denotes the ratio of the number of *first-blood* to the number of rounds in one match.

$$\mathbf{F}_{\text{fbp}}(\mathbf{i}) = \frac{\#(\mathbf{FK}(i))}{\#(\text{round})} \quad (32)$$

*Onetap percentage (otp)*: [C] *Onetap* denotes a head-shot fire event on an opponent that results in elimination without the use of sniper rifles, and where the inflicted damage is equal to or greater than 100 (the full health of a player). The *otp* represents the ratio of the number of *Onetap* instances to the number of times damage is inflicted by normal weapons.

$$\mathbf{ONETAP}(\mathbf{E}_{\text{kill}}^{i \rightarrow o^*}[k]) = \begin{cases} 1, & (\mathbf{E}_{\text{fire}}^i = \mathbf{E}_{\text{kill}}^{i \rightarrow o^*}[k]) \wedge (\mathbf{E}_{\text{damage}}^{i \rightarrow o^*} \geq 100) \\ 0, & \text{otherwise} \end{cases} \quad (33)$$

$$\mathbf{F}_{\text{otp}}(\mathbf{i}) = \frac{\sum_k \mathbf{ONETAP}(\mathbf{E}_{\text{kill}}^{i \rightarrow o^*}[k])}{\sum_n \mathbf{E}_{\text{damage} \wedge \text{wp}(i) \neq \text{sniper rifle}}^{i \rightarrow o^*}[n]} \quad (34)$$

*Occluder-penetration index (opi)*: [S] *Occluder-penetration* denotes the elimination event that happens when the victim is eliminated behind one layer or more layers of occluders by a penetrated bullet. The occluders are typically walls, players (namely wall bang), or smoke. *opi* refers to a weighted index that reflects the extent of the average occluder-penetration eliminations conducted by the player. The use of the number of rounds within the division aims to eliminate bias brought by that. In our case, the weights in  $\alpha_i$  are 0.5, 1, 2, 0.5 respectively.

$$\mathbf{F}_{\text{opi}}(\mathbf{i}) = \frac{\mathbf{W}_i \alpha_i}{\#(\text{round})} \quad (35)$$

$$\text{where } \alpha_i = \begin{bmatrix} w_1 \\ w_2 \\ w_3 \\ w_4 \end{bmatrix},$$

$\mathbf{W}_i = [\sum_k \mathbf{E}_{\text{kill} \wedge p(1)}^{i \rightarrow o^*}[k] \quad \sum_n \mathbf{E}_{\text{kill} \wedge p(2)}^{i \rightarrow o^*}[n] \quad \sum_m \mathbf{E}_{\text{kill} \wedge p(>2)}^{i \rightarrow o^*}[m] \quad \sum_j \mathbf{E}_{\text{kill} \wedge ts[j]}^{i \rightarrow o^*}]$   
*Blind kill percentage (bkp)*: [S] Denote the percentage of a player performing elimination while blinded. *bkp* refers to the ratio of the sum of elimination events where the attackers suffer a blinded effect to the number of eliminations.

$$\mathbf{F}_{\text{bkp}}(\mathbf{i}) = \frac{\sum_k \mathbf{E}_{\text{kill} \wedge \text{blind}}^{i \rightarrow o^*}[k]}{\sum_n \mathbf{E}_{\text{kill}}^{i \rightarrow o^*}[n]} \quad (36)$$

*Critical hit percentage (chp)*: [C] Denote the *critical hit* rate. *Critical hit* represents a successful damage event that applies to a particular hit group (typically, head) that deals more damage than a normal blow. *chp* refers to the ratio of the number of critical hits to the number of damage caused.

$$\mathbf{F}_{\text{chp}}(\mathbf{i}) = \frac{\sum_k \mathbf{E}_{\text{headshot}}^{i \rightarrow o^*}[k]}{\sum_n \mathbf{E}_{\text{damage}}^i[n]} \quad (37)$$

*Average kill per round (akpr)*: Denote the average number of eliminations per round by a player in a match.

$$\mathbf{F}_{\text{akpr}}(\mathbf{i}) = \frac{\sum_k \mathbf{E}_{\text{kill}}^{i \rightarrow o^*}[k]}{\#(\text{round})} \quad (38)$$

4) *Props utilization features*:

*Flash efficiency index (fei)*: [S] Denote how well a player utilizes the flash grenade. *fei* refers to the ratio of the total affection duration on the opponents minus that on the friendlies to the total affection duration.

$$\mathbf{F}_{\text{fei}}(\mathbf{i}) = \frac{\sum_k \mathbf{ELAPSE}(\mathbf{E}_{\text{blind}}^{i \rightarrow o^*}[k]) - \sum_m \mathbf{ELAPSE}(\mathbf{E}_{\text{blind}}^{i \rightarrow o^*}[m])}{\sum_n \mathbf{ELAPSE}(\mathbf{E}_{\text{blind}}^{i \rightarrow p^*}[n])} \quad (39)$$

*Props utilization index (pui)*: [S] Denote how frequently a player utilizes props such as a high-explosive grenade, Molotov or incendiary, smoke grenade, or flash grenade. *pui* refers to the ratio of the sum of a player and the number of times different grenades are used to a fixed constant which reflects the maximum number of grenades used within this match for all players.  $\rho$  denotes the maximum number of props a player is allowed to carry per round. In our case,  $\rho$  is 5.

$$\mathbf{F}_{\text{pui}}(\mathbf{i}) = \frac{\#(\mathbf{HEG}(i)) + \#(\mathbf{INC}(i)) + \#(\mathbf{SMK}(i)) + \#(\mathbf{FLS}(i))}{\#(\text{player}) \times \#(\text{round}) \times \rho} \quad (40)$$

## D. Temporal Features

1) *Engagement features*: Engagement features are extracted at each tick of the event occurrence. The introduction of the Engagement features is as follows:

### • Damage features:

- **tick** [C]: the tick number;
- **seconds** [C]: the time elapsed within a round in second;
- **attackerSteamID, victimSteamID** [C] : the ID of the player;
- **attackerSide, victimSide** [C]: the team side of the player;
- **attackerX, attackerY, attackerZ, victimX, victimY, victimZ** [C]: the X, Y, and Z location coordination in  $\mathbb{R}^3$  of the player;

- **attackerViewX**, **attackerViewY**, **victimViewX**, **victimViewY** [C]: the X and Y view direction coordination in  $\mathbb{R}^2$  of the player;
  - **attackerStrafe** [C]: the Boolean value indicates whether the attacker is moving sideways relative to their forward direction;
  - **weapon** [C]: the ID of the damage-caused weapon;
  - **weaponClass** [S]: the class ID of the damage-caused weapon;
  - **hpDamage** [C]: the value of damage caused to the victim;
  - **hpDamageTaken** [C]: the value of damage taken by the victim;
  - **armorDamage** [S]: the value of the damage caused to the victim’s armor;
  - **armorDamageTaken** [S]: the value of damage taken by the victim’s armor;
  - **hitGroup** [C]: the ID of the damage-taken area on the body of the victim;
  - **isFriendlyFire** [S]: the Boolean value indicates whether the damage is from the friendly;
  - **distance** [C]: the distance between the attacker and the victim;
  - **zoomLevel** [S]: the zoom level of the attacker’s weapon;
  - **roundNum** [S]: the round number of the current tick.
  - **Auxiliary props features**: The tick, second, IDs, sides, location, view direction, and round number are similar to above;
    - **flashDuration** [S]: the time elapsed for the blinding effect affects on the victim in seconds;
  - **Offensive props features**: The ID, side, location, view direction of the thrower and the prop, and round number are similar to above;
    - **throwTick**, **destroyTick** [S]: the tick of the prop thrown or destroyed;
    - **throwSeconds**, **destroySeconds** [S]: the time elapsed within a round in seconds at the moment of the prop thrown or destroyed;
  - **Elimination features**: The tick, second, IDs, sides, location, view direction, distance, weapon, weapon class, and round number are similar as above;
    - **assisterSteamID** [C]: the ID of the assister;
    - **assisterSide** [C]: the team side of the assister;
    - **isSuicide** [C]: the Boolean value indicates whether the elimination is a suicide event;
    - **isTeamkill** [S]: the Boolean value indicates whether the elimination is a team kill event;
    - **isWallbang** [S]: the Boolean value indicates whether the elimination is conducted by occluder penetration;
    - **penetratedObjects** [S]: the number of obstacles the bullet penetrated;
    - **isFirstKill** [C]: the Boolean value indicates whether the elimination is the first kill within a round;
  - **isHeadshot** [C]: the Boolean value indicates whether the elimination is a head-shot event;
  - **victimBlinded** [S]: the Boolean value indicates whether the victim is blinded;
  - **attackerBlinded** [S]: the Boolean value indicates whether the attacker is blinded;
  - **flashThrowerSteamID** [S]: the ID of the flash-thrower;
  - **flashThrowerSide** [S]: the team side of the flash-thrower;
  - **noScope** [S]: the Boolean value indicates whether the elimination is conducted with no scoped;
  - **thruSmoke** [S]: the Boolean value indicates whether the elimination is conducted through smoke;
  - **isTrade** [S]: the Boolean value indicates whether the elimination is traded with the opponent;
  - **Weapon fire features**: The IDs, sides, location, view direction, weapon, weapon class, player strafe, zoom level of the attacker, and the tick, second, and round number are similar as above;
    - **ammoInMagazine** [C]: the number of ammunition in the magazine;
    - **ammoInReserve** [C]: the number of ammunition in the reserve;
- 2) *Movement features*: Movement features are extracted per tick. The IDs, sides, location, view direction of the player, and the tick, second, and round numbers are similar to those above. The rest of the introduction of the Movement features is as follows:
- **velocityX**, **velocityY**, **velocityZ** [C]: the velocity of the player in 3D space;
  - **isAlive** [C]: the Boolean value indicates whether the player is alive;
  - **isBlinded** [S]: the Boolean value indicates whether the player is blinded;
  - **isAirborne** [S]: the Boolean value indicates whether the player is feet dangling;
  - **isDucking** [C]: the Boolean value indicates whether the player is ducking;
  - **isDuckingInProgress** [C]: the Boolean value indicates whether the player is ducking in progress;
  - **isUnDuckingInProgress** [C]: the Boolean value indicates whether the player is standing up from ducking in progress;
  - **isDefusing** [S]: the Boolean value indicates whether the player is defusing the bomb;
  - **isPlanting** [S]: the Boolean value indicates whether the player is planting the bomb;
  - **isReloading** [C]: the Boolean value indicates whether the player is reloading;
  - **isInBombZone** [S]: the Boolean value indicates whether the player is in the bomb planting area;
  - **isStanding** [C]: the Boolean value indicates whether the player is standing;

- **isScoped** [S]: the Boolean value indicates whether the player is scoped with the weapon;
- **isWalking** [S]: the Boolean value indicates whether the player is walking;
- **IsolationDegree** [C]: the distance to the calculation center of each teammate.

3) *Economy features*: Economy features are extracted per round. The introduction of the Economy features are as follows:

- **round** [S]: the number of round;
- **equipmentValueFreezetimeEnd** [S]: the value of the player's equipment after the end of the freeze time (the interval from the commencement of a round to the moment players are granted the ability to move and fire. This period typically allows players to purchase equipment);
- **equipmentValueRoundStart** [S]: the value of the player's equipment at the start of each round;
- **cash** [S]: the amount of money the player obtains at the end of each round;
- **cashSpendTotal** [S]: the amount of money the player spends within each round.

#### E. Sense and Performance Features Classification

All features presented in this section are recombinations of features from the first two subsystems, categorized into two main types, i.e., sense features and performance features. For a detailed description of each feature, please refer to [Section -D](#) and [Section -C](#). The following merely enumerates the specific categorizations of the features and some brief descriptions.

1) *Sense Features*: Sense features indicate a player's in-game cognition, emphasizing their strategic acumen and tactical foresight.

- **Temporal Sense Features**:
  - **Economy features**: Financial transactions and asset management, mirroring strategic resource allocation.
  - **Movement features**: Spatial patterns, positioning, and navigation dynamics, indicating tactical awareness.
  - **Flash features**: Strategic deployment of flash grenades during in-game engagements.
  - **Grenade features**: Utilization of assorted grenades, highlighting understanding of map control.
- **Structured Sense Features**:
  - **Flash efficiency index (fei)**: Metrics gauging flash grenade efficiency.
  - **Occluder-penetration index (opi)**: Achieve eliminations at specific locations, demonstrating proficiency with the map.
  - **Inertial shot percentage (isp)**: As a normal human being's habitual firing after destroying an opponent.
  - **Blind kill percentage (bkp)**: Eliminations executed under visual impairment.
  - **Props utilization index (pui)**: Metrics showcasing prop usage across the whole match.

2) *Performance Features*: Performance features encapsulate a player's in-game efficacy, concentrating on engagement aptitude, aiming precision, and mechanism mastery.

- **Temporal Performance Features**:

- **Elimination Features**: Efficiency of eliminations and some special, difficult eliminations.
- **Weapon Fire Features**: Proficiency metrics across weapon categories, illuminating combat adeptness.
- **Damage Features**: The player's performance with respect to inflicting effective damage in-game.

- **Structured Performance Features**: The remaining structured features in [Section -C](#).

#### F. PCA on Structured Features

In Section IV-A1, we have demonstrated the distribution distinction between cheaters and normal players. In the following section, we will demonstrate the PCA visualization on the structured features to display their orthogonality on both *Aimbot* and *Wallhack* datasets. [Figure 4](#) illustrates the structured features PCA results for both datasets regarding the cheaters and normal players respectively. Horizontal and vertical axes represent the first principal component (PC1) and the second principal component (PC2), respectively. These principal components capture the directions of maximum variance in the data, showing where the data varies most. The unit circle in a correlation circle plot is a circle with a radius of 1, serving as a reference. Within this circle, the vectors (represented as arrows) demonstrate the magnitude and direction of the original variables' associations with the principal components. The arrow represents feature vectors, where the direction and length of each arrow indicate the relationship of the original data features with the principal components. The direction of the arrow shows the correlation direction of the feature with the principal components. If two arrows are pointing in similar directions, it means their corresponding features exhibit similar patterns of variation in the dataset. Length indicates the impact or correlation strength of that feature on the corresponding principal component. Longer arrows suggest that the feature contributes more significantly to the variance captured by that principal component, and vice versa. It is noticeable that within the same plot, most of the features are distinct from others by obtaining different directions and lengths of the arrow. We can also observe that the direction and length of the arrows across *Aimbot* and *Wallhack* datasets are distinctive, indicating that the data distributions of the corresponding features are statistically different. Additionally, there are differences in the direction and length of the arrows between cheaters and normal players within the same or across different datasets. Above all, the original features can not be replaced by PCA.

#### G. Evaluation Metrics

The following are the detailed evaluation matrices that are used in Section VI.



**AUC-ROC**, denoted in Equation 47, is the area under the receiver operating characteristic curve, indicating the model's capability to differentiate between positive and negative classes. It is computed by integrating the ROC curve, as shown below, where  $TPR$  (True Positive Rate) is synonymous with Recall, and  $FPR$  (False Positive Rate) is defined in Equation 49.

$$AUC - ROC = \int_0^1 TPR(FPR) dFPR \quad (47)$$

**NPV**, shown in Equation 48, is the proportion of actual negative instances among all instances predicted as negative.

$$NPV = \frac{TN}{TN + FN} \quad (48)$$

**FPR**, indicated in Equation 49, is the proportion of actual negative instances that are incorrectly predicted as positive.

$$FPR = \frac{FP}{FP + TN} \quad (49)$$

#### REFERENCES

- [1] Tracker Network, "Tracker Network: Find your stats for your favorite games," <https://tracker.gg/>, 2024, Accessed: 2024-04-28.
- [2] D. Liu, X. Gao, M. Zhang, H. Wang, and A. Stavrou, "Detecting passive cheats in online games via performance-skillfulness inconsistency," in *2017 47th Annual IEEE/IFIP International Conference on Dependable Systems and Networks (DSN)*. Denver, CO, USA: IEEE, 2017, pp. 615–626.